Measurements of Slope Currents and Internal Tides on the Continental Shelf and Slope off Newport Beach, California

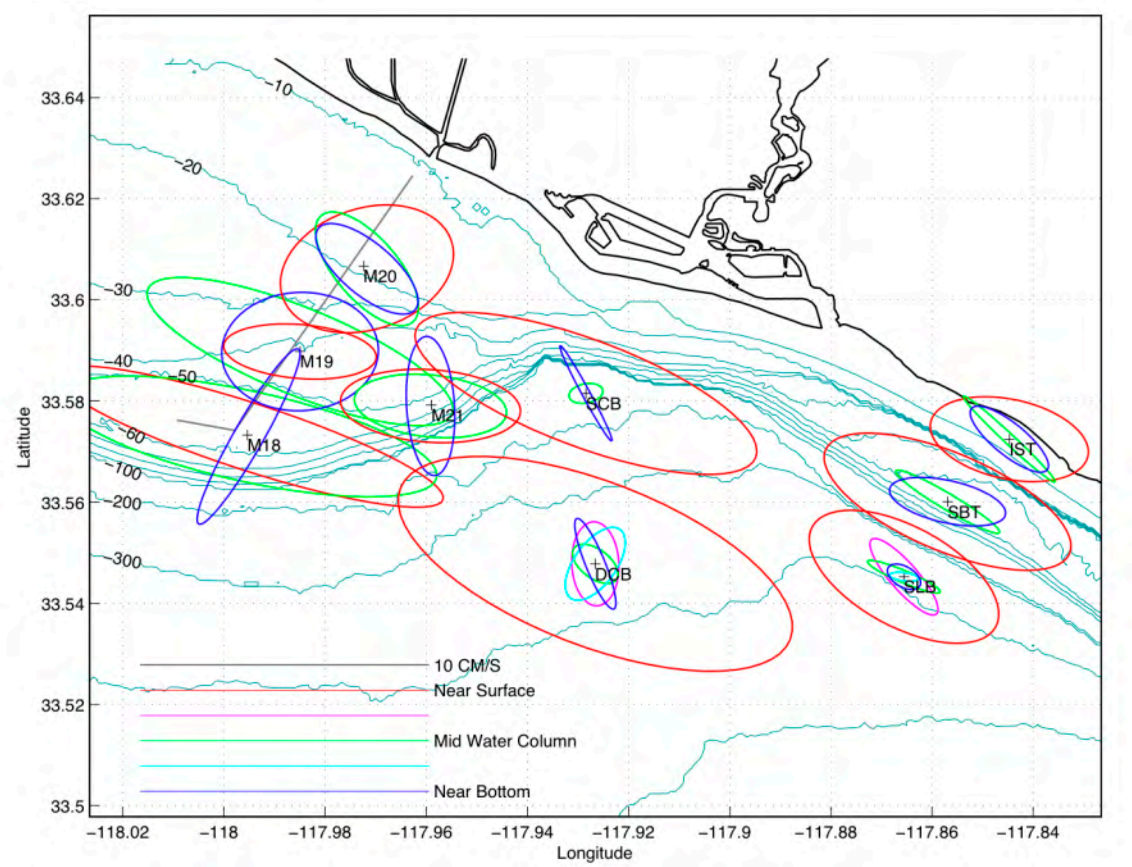

Open-File Report 2014–1041

U.S. Department of the Interior
U.S. Geological Survey

Measurements of Slope Currents and Internal Tides on the Continental Shelf and Slope off Newport Beach, California

By Kurt Rosenberger, Marlene A. Noble, and Benjamin K. Norris

Open-File Report 2014–1041

U.S. Department of the Interior
U.S. Geological Survey

U.S. Department of the Interior
SALLY JEWELL, Secretary

U.S. Geological Survey
Suzette M. Kimball, Acting Director

U.S. Geological Survey, Reston, Virginia: 2014

Suggested citation:
Rosenberger, Kurt, Noble, M.A. and Norris, B.K., 2013, Measurements of Slope Currents and Internal Tides on the Continental Shelf and Slope off Newport Beach, California: U.S. Geological Survey Open-File Report 2014–1041, 65 p., *http://dx.doi.org/10.3133/ofr20141041*.

ISSN 2331-1258 (online)

Contents

Figures

Tables

Conversion Factors

Inch/Pound to SI

Multiply	By	To obtain
	Length	
inch (in.)	2.54	centimeter (cm)
inch (in.)	25.4	millimeter (mm)
foot (ft)	0.3048	meter (m)
mile (mi)	1.609	kilometer (km)
mile, nautical (nmi)	1.852	kilometer (km)
yard (yd)	0.9144	meter (m)
	Flow rate	
foot per second (ft/s)	0.3048	meter per second (m/s)
cubic foot per second (ft^3/s)	0.02832	cubic meter per second (m^3/s)
mile per hour (mi/h)	1.609	kilometer per hour (km/h)
	Mass	
ounce, avoirdupois (oz)	28.35	gram (g)
pound, avoirdupois (lb)	0.4536	kilogram (kg)
	Pressure	
atmosphere, standard (atm)	101.3	kilopascal (kPa)
bar	100	kilopascal (kPa)
	Density	
pound per cubic foot (lb/ft^3)	16.02	kilogram per cubic meter (kg/m^3)
pound per cubic foot (lb/ft^3)	0.01602	gram per cubic centimeter (g/cm^3)

Measurements of Slope Currents and Internal Tides on the Continental Shelf and Slope off Newport Beach, California

By Kurt Rosenberger, Marlene A. Noble, and Benjamin K. Norris

Abstract

An array of seven moorings housing current meters and oceanographic sensors was deployed for 6 months at 5 sites on the Continental Shelf and slope off Newport Beach, California, from July 2011 to January 2012. Full water-column profiles of currents were acquired at all five sites, and a profile of water-column temperature was also acquired at two of the five sites for the duration of the deployment. In conjunction with this deployment, the Orange County Sanitation District deployed four bottom platforms with current meters on the San Pedro Shelf, and these meters provided water-column profiles of currents. The data from this program will provide the basis for an investigation of the interaction between the deep water flow over the slope and the internal tide on the Continental Shelf.

Introduction

In the summer of 2011, scientists of the U.S. Geological Survey (USGS) deployed seven moored platforms at five sites in the coastal ocean and slope off Newport Beach, California (fig. 1). The primary goal of the measurement program was to understand how internal tides on the narrow shelf to the south and east of Newport Beach differ from those previously observed on the wider shelf of San Pedro Bay (Noble and Xu, 2004), and subsequently, how sediment resuspension due to the internal tide may differ. Two secondary goals were (1) to understand how the internal tide on the shelf might be modulated by the flow over the slope, specifically by the California Undercurrent, and (2) to measure currents and sediment-transport events in Newport Canyon and to compare and contrast the flow and transport events in this canyon to those previously observed by USGS scientists in other canyons off the coast of California.

Concurrent with this measurement program, the Orange County Sanitation District (OCSD) placed four bottom platforms with acoustic Doppler current profilers on the San Pedro Shelf just to the north and west of Newport Beach, and the resulting data proved invaluable for comparison between the two shelves (fig. 1). The OCSD dataset consists of data from two deployments—the first was from May through October 2011, and the second was from October 2011 through January 2012. We present results from analyses of data collected during this second deployment period, when there is maximum overlap between the USGS and OCSD datasets.

Methods

Field Program

The following is a description of the instruments used in the program the platforms deployed at each site, the measurment goals, and which instruments were used to achieve those goals.

Instruments

Acoustic Doppler Current Profilers

An acoustic Doppler current profiler (ADCP) estimates current velocity in the water by sending an acoustic pulse into the water column and measuring the Doppler shift of the returned echo, which is reflected back by suspended particulate matter. The instrument can obtain a profile of current velocity by measuring the shift at different time lags, which correspond to different distances away from the instrument. The ADCPs used in this study, manufactured by Teledyne RD Instruments (TRDI), utilize proprietary broadband technology consisting of a pair of pulses sent together to achieve lower standard deviation of single pulses. This reduces the number of pulses per averaged ensemble required to attain a desired level of accuracy, thus allowing the user to collect ensembles at a higher sampling frequency. One disadvantage of the broadband technology, however, is that it reduces the overall profiling range of the instrument. The user has the option of setting the instrument in narrow-band mode to increase the range, at the expense of higher battery consumption, and thus the sampling frequency and (or) length of data record. One limitation of the ADCP, regardless of profiling mode, is that a certain percentage of the profile is potentially lost near boundaries, such as the surface or bottom, as a result of interference with side lobes of the acoustic beam. For the the TRDI ADCP used in this study, 6 percent of the water column is potentially affected.

Single-Point Acoustic Doppler Current Meter

A Nortek Aquadopp single-point acoustic Doppler current meter (AQD) was used on the surface buoy at each site to provide an independent measure of currents at the surface, where data on currents from the profiling ADCP could potentially be unusable. The Aquadopp also uses Doppler technology, by employing three acoustic beams to estimate water velocity at a single depth level.

Conductivity/Temperature Recorders

Conductivity/temperature (CT) recorders measure water temperature and conductivity at the sensor location and record the values at specified intervals. From these measurements, salinity can be calculated by using the 1978 Practical Salinity Scale (http://www.seabird.com/application_notes/AN14.htm) (IEEE, 1980).
Some CT recorders have the capability to log data from other sensors as well, such as pressure sensors, or analog external sensors that measure optical backscatter or fluorometry. A CT recorder with a pressure sensor installed (for measuring water depth) is referred to as a CTD.

Temperature Loggers

A temperature logger (thermistor) measures temperature and records the data at programmed intervals. Typically, the thermistor is mounted on the exterior of the underwater housing, such that the instrument may respond more rapidly to rapid changes in water temperature.

Optical Backscatter Sensors

An optical baskscatter sensor (OBS) measures turbidity by sending a beam of infrared light into the water and then measuring the quantity of light that is reflected back to its sensor from suspended particles. The relationship between the raw OBS signal and the suspended-sediment concentration can be determined in the laboratory by calibrating the sensors with sediment collected *in-situ*.

Transmissometers

A transmissometer measures the transmission of red collimated light (650 nm wavelength) from a light emitting diode (LED) along a fixed path through the water. Transmissometer data can be represented as a percentage of light transmission (from 0 to 100 percent, where 0 percent is completely occluded), or as light attenuation, or ‘beam-c’, in units of m^{-1} (utilizing another linear conversion). The advantage of presenting the data in light attenuation units is that the values increase as the suspended load increases. In addition, the usage of m^{-1} accounts for the path length of the instrument, thus making measurements from instruments of two different path lengths comparable.

Mooring and Instrument Setup

Of the five USGS mooring sites, three were arranged in a cross-shelf transect from the slope up onto the shelf southeast of Newport Harbor (referred to here as the Newport Shelf), and two were in Newport Canyon (fig. 1, table 1). The shallowest site of the Newport Shelf array consisted of a tripod and surface-mooring pair in 15 m water depth, referred to here as the Inner Shelf site (fig. 2). The tripod (mooring ID NPT11IST) housed a 1,200-kHz TRDI Workhorse ADCP for measuring water-column profiles of currents and surface waves, a CTD that logged two LED transmissometers and a dissolved-oxygen sensor, and a second CTD for comparative purposes. The surface mooring (mooring ID NPT11ISS) housed a CTD, a single-point current meter positioned 1 m below the surface and a wind sensor for measuring windspeed and direction 2 m above the surface.

The two CTDs on the tripod use different methods for estimating the salinity of the water; the first measures conducitivity with an inductive coil, and the second measures conducitivity with an electrode conductivity cell. In addition, each transmissometer had a different mechanism for preventing fouling. The first transmissiometer (variable ATTN1) measured light attenuation through a volume of water in an enclosed flow-though tube that was connected to a plumbed system driven by the CTD pump. Incoming water samples to this transmissometer first passed through the CTD conductivity cell, and thus contain trace amounts antifoulant that should adequately prevent growth on the sensor face of the tranmissometer. The second transmissometer (variable ATTN2) was an open system that had an automated wiper, with brushes designed to wipe the sensor face clean on regular intervals.

Table 1. List of moorings deployed, measurement goals, and deployment times and locations at the five study sites, Newport Beach, California.

Site	Platform	Measurement Goal	Latitude (North)	Longitude (West)	Depth (m)	Deployed (GMT)	Recovered (GMT)
NPT11IST Inner Shelf	Small Tripod	Currents, suspended sediment, waves	33.572	117.845	14.2	7/21/2011, 15:16:40	1/24/2012, 14:58:00
NPT11ISS Inner Shelf	Surface Buoy	Winds, surface currents, temperature	33.572	117.844	15.2	7/21/2011, 14:55:20	1/25/2012, 16:21:15
NPT11SBT Shelf Break	Small Tripod	Currents, suspended sediment	33.560	117.857	85.2	7/20/2011, 16:39:00	1/24/2012, 16:18:00
NPT11SBS Shelf Break	Surface Mooring	Winds, surface currents, water column temperature	33.559	117.857	83.0	7/20/2011, 16:08:00	1/24/2012, 18:13:00

Site	Platform	Measurement Goal	Latitude (North)	Longitude (West)	Depth (m)	Deployed (GMT)	Recovered (GMT)
NPT11SLB Slope	Sub-Surface Mooring	Water Column Currents and temperature, suspended sediment	33.545	117.866	358.0	7/18/2011, 23:57:00	3/20/2012, 16:00:00
NPT11DCB Deep Canyon	Sub-Surface Mooring	Water Column Currents, suspended sediment	33.548	117.927	390.0	7/18/2011, 15:10:00	1/25/2012, 21:00:00
NPT11SCB Shallow Canyon	Sub-Surface Mooring	Water Column Currents, suspended sediment	33.582	117.928	215.0	7/18/2011, 20:00:00	1/25/2012, 15:06
HBC11M18	Small Tripod	Water Column Currents	33.573	117.995	58.0	10/24/2011, 18:50:00	1/27/2012, 18:25:30
HBC11M19	Small Tripod	Water Column Currents	33.590	117.984	40.0	10/24/2011, 17:49:00	1/27/2012, 19:01:00
HBC11M20	Small Tripod	Water Column Currents	33.607	117.972	20.0	10/26/2011, 19:25:00	1/27/2012, 19:25:00
HBC11M21	Small Tripod	Water Column Currents	33.579	117.959	56.0	10/26/2011, 17:31:00	1/27/2012, 18:13:30

Offshore of the Inner Shelf site, another bottom mounted tripod and surface-mooring pair were deployed on the shelf break in 85 m water depth, referred to here as the Shelf Break site (fig. 3). The tripod (mooring ID NPT11SBT) housed a 300-kHz RDI Workhorse ADCP that profiled the entire water column and a CTD that logged measurements of temperature, salinity, and light attenuation by using an external LED transmissometer. In addition, the tripod housed a broadband 5-beam ADCP for measuring high-resolution profiles of currents in the first 4 m above the tripod. The surface mooring (mooring ID NPT11SBS) had thermistors on the mooring wire at 10-m intervals, and the surface buoy housed a CTD, a single point current meter for measuring at 1 m water depth, and a wind sensor for measuring windspeed and direction 3 m above the surface.

The deepest site of the Newport Shelf mooring array lay on the slope at about 350 m water depth, and consisted of one 247-m-tall subsurface mooring (mooring ID NPT11SLB), referred to here as the Slope mooring. This mooring had three 300-kHz RDI Workhorse ADCPs arranged vertically to measure currents throughout the water column, as well as a string of thermistors at 25-m intervals along the mooring wire (fig. 4). A CTD in an in-line frame 19 above the bed, logged light-attenuation data from an LED transmissometer. The purpose of this mooring was to detect the presence of the California Undercurrent in this region and to observe internal tides propogating onto the Newport Shelf.

Two of the three ADCPs on the Slope mooring were mounted in an upward and downward configuration in a subsurface sphere at the top of the mooring at 170 m water depth. These two instruments were programmed in narrowband (or long-range) mode, with 4-m vertical bins, to acquire longer current profiles than could be achieved with the standard broadband mode. The assumed maximum range for each was 150 m, thus covering 300 m of the water column. A Seabird SBE-39 pressure and temperature recorder was also placed on the ADCP frame to monitor laydown of the mooring due to strong currents. The third ADCP was placed in a downward configuration measuring in standard broadband mode with smaller, 2-m bins, to provide more accurate measurements of near-bottom flow. This ADCP was conservatively placed 80 m above the bed, as the maximum range in this mode is 100 m. The planned water depth for this mooring was 380 m, and in anticipation that the long-range ADCPs might not acquire data to the full extent specified by the manufacturer, a known gap between measurement volumes was built into the mooring design between the middle ADCP and the lower ADCP.

Two subsurface moorings were deployed in Newport Canyon to assess the potential for transport of sediment from the shelf down-canyon to the continental slope and rise. The deeper of the two moorings (mooring ID NPT11SLB) was of a similar configuration to that of the Slope mooring, except that it was shorter, at 217 m in height. It was deployed in 390 m water depth with three 300-kHz TRDI Workhorse ADCPs in a vertical configuration that collected profiles of current velocities throughout the water column (fig. 5). Although this mooring did not have a full string of thermistors as the Slope mooring did, there was a high-resolution thermistor on each ADCP frame and a Seabird SBE-37 CT logger and an RBR Branker logger recording measurements from a Wetlabs C-Star 25-cm transmissometer in a frame 19 mab. The canyon has slight relief at this water depth (that is, the canyon itself is not deep); the rim of the canyon is approximately 30 m above the canyon floor (fig. 1).

A shorter, 90-m-tall mooring was deployed in the shallower section of Newport Canyon in 215 m water depth (mooring ID NPT11SCB). This mooring consisted of two 300-kHz RDI Workhorse ADCPs in a paired upward-downward configuration to acquire profiles of currents throughout the entire water column (fig. 6). The downward-facing ADCP was programmed to broadband mode, collecting current data in 2-m vertical bins every 5 minutes, in order to better resolve the near-bed flows and any potential turbidity currents. The upward-facing ADCP was programmed in narrow-band mode, collecting profiles in 4-m vertical bins every 15 minutes. A Seabird SBE-39 pressure and temperature recorder was also placed on the ADCP frame to monitor laydown of the mooring due to strong currents. An SBE-16 CTD in an in-line mooring frame, 21 meters above bottom, measured temperature, salinity and pressure and logged data from a Wetlabs C-Star 10-cm transmissometer.

The OCSD dataset is presented here with permission from OCSD. The four sites occupied by OCSD during the USGS measurement program (M18, M19, M20, and M21) have been used by OCSD for many years to understand the flow on the San Pedro Shelf (SAIC, 2009). The USGS mooring IDs for these sites are HBC11M18, HBC11M19, HBC11M20 and HBC11M21. Each site consisted of an upward-facing ADCP mounted on a small, bottom tripod, approximately 1 mab; the first three sites had 300-kHz RDI Workhorse ADCPs, and the last site, HBC11M20, in shallower water, had a 600-kHz RDI ADCP. The measurement program consisted of two deployments; the first lasted 5 months from late-May until mid-October 2011, and the second lasted 3 months from late October 2011 until late January 2012. We present data from the second deployment only in this report, because this period had greater overlap with the USGS deployment.

Data Processing

Data-File Identifiers and Formats

An eight-character alpha-numeric mooring identification number (mooring ID) is assigned to each mooring or tripod and is used to identify all files containing time-series data recorded by instruments mounted on that platform. The mooring ID is the key to identifying and(or) locating data records in the USGS Pacific Coastal & Marine Science Center (PCMSC) time-series data-management system. In this identification scheme, the first three characters denote the project (in this case, ‘NPT’ for Newport Shelf), the next two characters identifiy the year, and the last three characters denote the site name and platform type. For example, NPT11IST denotes the Newport 2011 project Inner Shelf Tripod. Each instrument placed on the platform is then given a two-digit identifier, usually numbered according to the vertical position on the mooring or tripod. This two-digit identifier is appended to the end of each mooring ID to provide unique identifier for every instrument deployed in the ocean by PCMSC. Thus, NPT11IST01 identifies the topmost instrument on mooring NPT11IST; NPT11IST02 identifies the next instrument down on mooring NPT11IST, and so on. As data files are processed, additional identifiers are added to the ten-digit identifier to indicate sensors and any additional processing steps, such as averaging, that have been performed on the data. Table 2 summarizes the file-naming system.

Raw data files downloaded from each instrument were translated from the manufacturer's data format into the netCDF data-file format using instrument-specific toolboxes developed in Matlab by USGS scientists. The netCDF data file format, developed by the Unidata Corporation (http://www.unidata.ucar.edu/software/netcdf/), is a compact binary format compatible with most computer systems that stores both the data and the metadata in the file.

Table 2. Summary of U.S. Geological Survey netCDF file-naming conventions.

Mooring ID	Instrument Identifier	Sampling Scheme (optional)	Data Type (optional)	Version	File Extension
USGS Instrument ID	First three digits identify program, next two digits the year, next three digits the site name, and last two the instrument number.				
	mc	MicroCat temperature and salinity data			
	adc	ADCP water flow data			
	adv	ADV and accessory sensor data			
	pca	PCADP and accessory sensor data			
	abs	ABS statistics data			
	bt	Brancker temperature data			
	sc	Seacat temperature and salinity data			
	att	Transmissometer data			
		1	First sampling scheme when multiple schemes are used		
		2	Second sampling scheme when multiple scheme are used		
			b	Burst data for instruments with burst and statistics files	
			q	Quality data for instruments with flagging recorded in separate files	
				-a	USGS best basic version
					.nc netCDF file extension

Example file names

Instrument ID	Instrument Identifier	Sampling Scheme (optional)	Data Type (optional)	Version	File Extension
NPT11SLB15	bl			-a	.nc

.nc

Instrument ID	Instrument Identifier	Sampling Scheme (optional)	Data Type (optional)	Version	File Extension
NPT11IST01	wh		Wvs-p	-a	.nc

The USGS uses the Equatorial Pacific Information Collection conventions for organizing and naming oceanographic data variables developed by the National Oceanic and Atmospheric

Administration Pacific Marine Environmental Laboratory. The data were processed using quality-control procedures developed for all oceanographic data by the USGS. Files generated during the first processing step (which involved conversion to engineering units and quality-assurance calculations) were stored in netCDF format with '.cdf' suffixes. Subsequent data-processing steps can include the application of calibration coefficients, coordinate transformations, rotation into geographic coordinates, and averaging of good data. Final versions of the processed data variables are stored in netCDF format with '.nc' extensions. All of the final statistics data are in EPIC-compliant netCDF format.

Time

Times are reported in Universal Time [(UT, equivalent to Greenwich Mean Time (GMT)]. We checked for drift of instrument clocks by comparing instrument times with accurate times [(from the GPS, or from clocks synchronized with the National Institute of Standards and Technology in Boulder, Colorado (http://tf.nist.gov/)], before and after deployments. The observed offsets were small compared to the sample intervals (typically ~10), so no adjustments to any instrument times in this data set were made.

Time is recorded in the netCDF files as two variables, named time1 and time2, in compliance with EPIC standards to allow precise storage of time in integer format. Time1 is the Julian day, where midnight on May 23, 1968, equals 2,440,000, and time2 is the elapsed time on that day, in milliseconds since midnight. Thus, time in decimal Julian days is computed as time1+time2/(1,000 x 3,600 x 24).

Current-meter Data

Instrument Orientations

Each of the current meters had internally mounted flux-gate compasses. These compasses were calibrated prior to deployment according to manufacturer's recommendations. Raw current data were recorded in beam coordinates for instruments mounted on the bottom (that is, they were not freely moving) and the data were transformed into earth coordinates (corrected for pitch, roll, and heading) during post processing. Velocity data was recorded in earth coordinates for instruments mounted on subsurface or surface moorings, whereby the instrument performs the coordinate transformation in real time for each ensemble. It was necessary to do this for these moorings because the frames on the mooring lines were able to rotate and pitch.

All data were rotated to true geographic coordinates (positive axes toward east, north, and up) using instrument compasses and tilt sensors and correcting for local magnetic variation (12.4º east of true North). For some of the results and discussions, the horizontal components of current velocity have been rotated into alongshore and cross-shore coordinates, with the positive alongshore axis oriented toward 300º True. Flow in the positive alongshore direction (toward Los Angeles) is described as upcoast or poleward, whereas flow in the negative alongshore direction (toward San Diego) is described as downcoast or equatorward.

Acoustic Doppler Current Profiler Data

The ADCP data were processed according to standard USGS procedures by using ADCP Tools, a collection of Matlab routines written to read in and process raw ADCP data and to create netCDF files of the raw and processed data. The toolbox is described in USGS Open-File Report 00–458. Raw data files from the ADCPs were converted to netCDF format and checked for clock accuracy by comparing in-and-out-of-water times to the mooring log and checking for linear-time progression. Data were despiked, with gaps replacing bad data points. The clocks, ADCP calibrations, and internal compasses of nearby instruments were compared for consistency. Automatic algorithms were used to check for high-intensity reflection indicative of fish or other beam obstructions. Bad values were masked both manually and automatically and, where possible, a three-beam solution was used to fill in gaps caused by one compromised beam. Data above the water surface were masked; since the water depth at the site varies with the stage of the tide, there are periods when some bins above the water surface are retained within the file. Data collected before the instrument was on bottom or after it was recovered were trimmed. Finally, the data were rotated from beam coordinates into geographic coordinates. The final processed versions of these data were stored in EPIC-compliant netCDF format.

Aquadopp Single-point Current-meter Data

Raw current-velocity data measured by the Aquadopp single-point current meters were first converted into netCDF format These instruments were set to record velocity data in Earth coordinates as while they were mounted on freely-rotating surface platforms. The data were screened for quality using standard thresholds for acoustic correllation and return-echo intensity, and then they were rotated into geographic coordinates using the local magnetic variation.

Optical Backscatter Sensor Data

The Nortek Aquadopp data logger converts raw optical backscatter sensor (OBS) voltage measurements to counts with a 16-bit analog-digital converter. Data were converted from counts back to volts (a linear conversion) in the processing so that the data could be calibrated to sediment concentration using laboratory-derived calibration coefficients. The Seabird SBE-16 Seacat logs the analog voltages from the OBS directly. The data are available in the netCDF '.nc' file for the instrument to which the OBS was connected (Seabird Seacat or Nortek Aquadopp). As there are no standards for screening bad data values for this data type, no quality/-control procedure has been applied, and determining quality of the data is at the discretion of the researcher.

Transmissometer Data

Seabird SeaCAT CTD loggers and RBR Brancker loggers were used to log raw voltage data from the transmissometers. Processing of the data from these loggers includes converting the raw voltage values into values of light attenuation (beam-c) in units of m^{-1}. The final data are available in the .nc file for the instrument with which the transmissometer was deployed (RBR Branker logger or Seacat).

Results

Data Return

The following is a discussion of the data return for each platform deployed. A detailed listing of the data return for each instrument is provided in table 3, and a timeline of the data return (for USGS data only) by data type and platform is presented in figure 7.

Inner Shelf Site

The tripod at the Inner Shelf site (NPT11IST) collected a complete record of water-column currents and waves (as recorded by the ADCP) and water properties (temperature and salinity) from one CTD. A second CTD that was logging data from two transmissometers and an oxygen sensor stopped recording on November 14, 2011. Low-pass, filtered (to remove tidal fluctuations) alongshore and cross-shore current velocity data from three depth levels are plotted in figure 8, and directional-wave parameters are plotted in figure 9. Water properties, as measured by the two CTDs on the tripod and measurements of light attenuation (made by the two individual transmissometers), are plotted in figure 10.

Table 3. Detailed listing of data return for each instrument. Values for depth(s) listed represent the depth(s) that the instrument made measurements, not necessarily the depth of the instrument itself.

[Abbreviations of parameters: T, temperature; S, salinity; SS, suspended sediment; CP, current profile; D, directional wave data; W, non-directional wave data; Met, meteorologic data]

Mooring	Instrument	Depth (Height)	Parameters Measured	Sampling Scheme	Processed File(s)	Date Ranges
NPT11IST - Inner Shelf Tripod - 15.2m						
NPT11IST01	RDI 1200 kHz ADCP	2.4-14.4	CP/T/W	3 minute	NPT11IST01wh.nc	7/21/11-1/24/12
NPT11IST02	RBR XR-420 CTD	14.1	S/T/D	5 minute	NPT11IST02ctd.nc	7/21/11-1/24/12
NPT11IST03	Seabird SBE-16+/Trans/OBS	14.4	CP/T	6 minute	NPT11IST03sc.nc	7/21/11-11/14/11
NPT11ISS - Inner Shelf Surface Mooring - 14.3m						
NPT11ISS01	Airmar Met PB-200	2	Met	3 minute	NPT11ISS01met.nc	11/12/11-1/24/12
NPT11ISS02	RBR XR-420 CTD	1	S/T/D	5 minute	NPT11ISS02ctd.nc	7/21/11-1/2/12
NPT11ISS03	Nortek Current Meter	1	CP/T	3 minute	NPT11ISS03aq-cal.nc	7/21/11-1/24/12
NPT11SBS - Shelf Break Surface Buoy - 83m						
NPT11SBS01	Airmar Met PB-200	2	Met	3 minute	NPT11SBS01met.nc	7/20/11-7/31/11
NPT11SBS02	RBR XR-420 CTD	1	S/T/D	5 minute	NPT11SBS02ctd.nc	7/20/11-1/24/12
NPT11SBS03	Nortek Current Meter	1	CP/T	3 minute	NPT11SBS03aq-cal.nc	7/20/11-1/24/12
NPT11SBS04	RBR TR-1050 Temperature	10	T	1 minute	NPT11SBS04bt.nc	7/20/11-1/24/12
NPT11SBS05	RBR TR-1050 Temperature	20	T	1 minute	NPT11SBS05bt.nc	7/20/11-1/24/12
NPT11SBS06	RBR TR-1050 Temperature	30	T	1 minute	NPT11SBS06bt.nc	7/20/11-1/24/12
NPT11SBS07	RBR TR-1050 Temperature	40	T	1 minute	NPT11SBS07bt.nc	7/20/11-1/24/12
NPT11SBS08	RBR TR-1050 Temperature	50	T	1 minute	NPT11SBS08bt.nc	7/20/11-1/24/12
NPT11SBS09	RBR TR-1050 Temperature	60	T	1 minute	NPT11SBS09bt.nc	7/20/11-1/24/12
NPT11SBS10	RBR TR-1050 Temperature	70	T	1 minute	NPT11SBS10bt.nc	7/20/11-1/24/12
NPT11SBS11	RBR TR-1050 Temperature	80	T	1 minute	NPT11SBS11bt.nc	7/20/11-1/24/12
NPT11SBT - Shelf Break Tripod - 85.2m						
NPT11SBT01	RDI 300 kHz ADCP	9.2-81.2	CP/T	3 minute	NPT11SBT01wh.nc	7/20/11-1/24/12
NPT11SBT02	RDI 1200 kHz 5-Beam BBADCP	84	CP/T	7.5min bursts		
NPT11SBT03	Seabird SBE-16+/Trans/OBS	84	S/T/D/SS	5 minute	NPT11SBT03sc.nc	7/20/11-1/24/12
NPT11SLB - Slope Subsurface Mooring - 358m						
NPT11SLB01	RDI 300 kHz ADCP	6.8-	CP/T	15 minute	NPT11SLB01wh.nc	7/19/11-12/23/12

Mooring	Instrument	Depth (Height)	Parameters Measured	Sampling Scheme	Processed File(s)	Date Ranges
		106.8				
NPT11SLB02	Seabird SBE-39 TP	97	T/CP	5 minute	NPT11SLB02pr.nc	7/19/11-3/20/12
NPT11SLB03	RDI 300 kHz ADCP	119.1-275.1	CP/T	15 minute	NPT11SLB03wh.nc	7/19/11-12/23/12
NPT11SLB04	Star Oddi Temperature	117	T	1 minute	NPT11SLB04st.nc	7/19/11-3/18/12
NPT11SLB05	Star Oddi Temperature	142	T	1 minute	NPT11SLB05st.nc	7/19/11-3/18/12
NPT11SLB06	Star Oddi Temperature	167	T	1 minute	NPT11SLB06st.nc	7/19/11-3/18/12
NPT11SLB07	Star Oddi Temperature	192	T	1 minute	NPT11SLB07st.nc	7/19/11-3/20/12
NPT11SLB08	Star Oddi Temperature	217	T	1 minute	NPT11SLB08st.nc	7/19/11-3/18/12
NPT11SLB09	Star Oddi Temperature	242	T	1 minute	NPT11SLB09st.nc	7/19/11-3/18/12
NPT11SLB10	Star Oddi Temperature	267	T	1 minute	NPT11SLB10st.nc	7/19/11-3/18/12
NPT11SLB11	RDI 300 kHz ADCP	292.2-354.2	CP/T	15 minute	NPT11SLB11wh.nc	7/19/11-3/20/12
NPT11SLB12	RBR TR-1050 Temperature	272	T	1 minute	NPT11SLB12bt.nc	7/18/11-3/20/12
NPT11SLB13	Star Oddi Temperature	292	T	1 minute	NPT11SLB13st.nc	7/18/11-3/20/12
NPT11SLB14	Star Oddi Temperature	317	T	1 minute	NPT11SLB14st.nc	7/18/11-3/20/12
NPT11SLB15	RBR Logger/ Seatech Trans	323	SS	10 minute	NPT11SLB15bl.nc	7/18/11-2/29/12
NPT11SLB16	Seabird SBE-37 CT	323	S/T	5 minute	NPT11SLB16mc.nc	7/19/11-3/18/12
NPT11DCB - Deep Canyon Subsurface Mooring - 390m						
NPT11DCB01	RDI 300 kHz ADCP	10.8-166.8	T/S	15 minute	NPT11DCB01wh.nc	7/18/11-1/25/12
NPT11DCB02	Seabird SBE-39 TP	173	T/CP	3 minute	NPT11DCB02pr.nc	7/19/11-1/25/12
NPT11DCB03	RDI 300 kHz ADCP	174.1-330.1	T/S	15 minute	NPT11DCB03wh.nc	7/18/11-1/25/12
NPT11DCB04	RDI 300 kHz ADCP	324.2-386.2	T	15 minute	NPT11DCB04wh.nc	7/18/11-1/25/12
NPT11DCB05	RBR TR-1050 Temperature	320	T	3 minute	NPT11DCB05bt.nc	7/18/11-1/25/12
NPT11DCB06	Seabird SBE-37 CT	371	T/S	3 minute	NPT11DCB06mc.nc	7/19/11-1/25/12
NPT11DCB07	RBR Logger/ Seatech Trans	371	T	3 minute	NPT11DCB07bl.nc	7/18/11-1/25/12
NPT11SCB - Shallow Canyon Subsurface Mooring - 215m						
NPT11SCB01	RDI 300 kHz ADCP	12.8-136.8	CP/T	15 minute	NPT11SCB01wh.nc	7/18/11-1/25/12
NPT11SCB02	Seabird SBE-39 TP	144	T/CP	5 minute	NPT11SCB02pr.nc	7/19/11-1/25/12
NPT11SCB03	RDI 300 kHz ADCP	147.2-205.2	CP/T	15 minute	NPT11SCB03wh.nc	7/18/11-11/1/11
NPT11SCB04	Seabird SBE-16 CT	187	S/T	5 minute	NPT11SCB04sc-aq.nc	7/18/11-1/25/12
NPT11SCB05	Sequoia LISST-25	187	SS	5 minute	NPT11SCB05ls.nc	

The instrumentation on the surface mooring at the Inner Shelf site (NPT11ISS) collected a mostly complete record for the deployment period. The meteorological station data logger did not record time for the first few months of the deployment, rendering those data unusable. The data logger began recording time on November 18, 2011, and continued through the end of the deployment period (fig. 11). The single-point Aquadopp current meter acquired a complete record of currents and optical backscatter, and the CTD recorded water properites through January 2, 2012 (fig. 12).

Shelf Break Site

The ADCP and the CTD on the Shelf Break tripod (NPT11SBT) collected data for the entire deployment period. The high-resolution ADCP collected burst data on currents for one month, however the data are not presented here because they are experimental. Low-pass filtered alongshore and cross-shore current velocity data from three depth levels are plotted in figure 13. Water properties (temperature and salinity), light attenuation, and optical backscatter data are plotted in figure 14.

The surface mooring at the Shelf Break site (NPT11SBS) collected a complete record of near-surface currents, temperature, and salinity (fig. 15), as well as water-column temperature data (figs. 16 and 17). The meteorological station at this site stopped recording data after one week; therefore, the data are not presented here.

Slope Site

The mooring at the Slope site (NPT11SLB) did not return to the surface when the initial recovery was attempted in January 2012; subsequently, USGS personnel returned to the site in March 2012 to recover the mooring with grappling hooks. Although this mooring collected a longer dataset than the rest, some instruments stopped prior to recovery as a result of battery failure, including the two ADCPs in the upper water column (both stopped on December 24, 2011) and the bottom transmissometer logger (NPT11SLB15, ending on February 29, 2012). All other instruments collected a full record for the duration of the deployment.

Low-pass filtered alongshore and cross-shore currents at several depth levels from the three ADCPs are plotted in figure 18, and near-bottom water properties (temperature and salinity) and light attenuation data are plotted in figure 19. Raw temperature readings from the thermistor string, ranging from 97 to 323 m water depth are shown in figure 20, and a contour plot of these data is presented in figure 21.

Shallow Canyon Site

The mooring placed in the shallow section of Newport Canyon (NPT11SCB) collected a complete record of currents and water properties for the deployment period. The upward facing ADCP collected water-column velocity data from 126 m water depth to the surface in 4 m vertical bins, while the downward facing ADCP collected velocity data from 136 m water depth to the bottom of the canyon at 194 m in 2 m bins. Low-pass, filtered current-meter data, rotated into alongshore and cross-shore orientations at several depth bins through the water column are plotted in figure 22. Data from the CTD/transmissometer package 17 m off the bottom and from the pressure/temperature logger mounted on the ADCP frame are plotted in figure 23.

Deep Canyon Site

The mooring placed in the deeper section of Newport Canyon (NPT11DCB) collected a complete record of currents and water properties for the deployment period. The top ADCP collected current data from 10 to 166 m water depth, the middle ADCP collected data from 180 to 324 m water depth (both in 4 m vertical bins), and the bottom ADCP collected data from 318 to 380 m water depth (in 2 m vertical bins). Low-pass filtered alongshore and cross-shore currents at several depth bins throughout the water column are plotted in figure 24. Data from the CTD/transmissometer package 17 m off the bottom and from as well as the pressure/temperature logger mounted on the ADCP frame are plotted in figure 25.

Ancillary Data

Data from other agencies were gathered for analysis in conjunction with the USGS data. Meteorological and wave data for the deployment period were acquired from NOAA buoy 46025, 33 nautical miles west-southwest of Santa Monica, in the Santa Monica Basin (http://www.ndbc.noaa.gov/station_page.php?station=46025) (figs. 26 and 27). Wind data on shore were acquired from two sources: (1) the OCSD Plant 2 near Talbot Marsh, and (2) a personal weather station on the Balboa Penisula at the entrance to Newport Harbor, downloaded from Weather Underground (http://classic.wunderground.com/weatherstation/WXDailyHistory.asp?ID=KCANEWPO17) (fig. 28). River discharge data were acquired from USGS streamflow-gaging station 11074000 on the Santa Ana River (2001) and were plotted in figure 29. We also obtained data on mean sea level for the duration of the deployment from NOAA’s National Ocean Service water-level station number 9410660 at the entrance to Los Angeles Harbor (http://co-ops.nos.noaa.gov/waterlevels.html?id=9410660).

Discussion

An assesment of the data quality involves an examination of basic statistics and standard oceanographic parameters to place the data in context with data previously acquired from the region and our current undertstanding of the important oceanographic processes. Here we focus on examining the profiles of current-meter data, the primary objective of this study.

Basic Statistics

Basic statistics were run on the current meter data to assess data quality and to compare to other available data (in particular, the OCSD current meter-data). The current-meter data are stored in the final format as eastward and northward vector components, and mean profiles of these components were computed for the entire deployment period. Alongshore and cross-shore components of the data were determined by rotating the current data to align with the coastline. This is often done individually for each moored platform, however for this presentation of the data, a single rotation value of 60 degrees was used to rotate all of the data into alongshore and cross-shore constituents. Profiles of mean alongshore and cross-shore velocity and speed and direction for the five USGS sites and the four OCSD sites are plotted in figures 30–38.

Mean flow through the region is predominantly poleward (upcoast) at depth and equatorward (downcoast) near the surface, as has been observed in previous studies in the central southern California Bight (Noble and Xu, 2004; Hamilton and others, 2006; Noble and others 2009; Rosenberger and others, 2011). The depth of the surface layer that flows downcoast (as well as the percentage of the water column) varies with distance from shore. On the San Pedro Shelf, the surface layer is 9 m deep (42 percent of the water column) inshore at site M20 (fig. 37) and 12 m deep (21 percent of the water column) at the southwestern end of the shelf at site M21 (fig 38), but it is not present mid-shelf (site M19) or at the southern end of the shelf (site M18). Both the Shallow Canyon and Deep Canyon sites exhibit downcoast flow at the surface that is 25 m deep (12 percent) and 50 m deep (13 percent), respectively. On the Newport Shelf to the southeast, most of the water column flows downcoast in 14 m water depth at the Inshore site (90 percent). Farther offshore this surface layer is 30 m deep (35 percent) at the Shelf Break site and ~45 m deep (13 percent) at the Slope site.

A slight discontinuity in current direction, at ~110 m water depth at the Slope site (fig. 32) and at ~175 m water depth at the Deep Canyon site (fig. 34), suggest suggests a slight difference in compass-direction readings between the upward-looking and downward-looking ADCP’s at each site. Although the compass for each instrument is calibrated for magnetic- field disturbance (primarily by the internal battery) at the beginning of the deployment, that disturbance can change over time as the battery is depleted. Unfortunately there is no way to account for this change, however, the difference is minor.

In addition to the profiles of the mean alongshore and cross-shore currents, it is instructive to examine the variance of the low-pass filtered (subtidal) data to ensure the patterns match the expected flow in the region. To achieve this we performed a principal components analysis (PCA) on the low-pass, filtered vector data, which resulted in ellipse parameters of the data variance (elucidating the primary orientation of the low-pass, filtered flow, the inclination of the major axis). PCA ellipses at several depths in the water column at each site are plotted in figure 39.

The PCA current ellipses are consistent with results from other measurement programs in the region (Hamilton and others, 2006; Rosenberger and others, 2011), demonstrating that the near-bottom current ellipses orient with the bathymetry, whereas the near-surface ellipses orient with the general trend of the coastline. The near-bottom ellipses the Shallow Canyon and Deep Canyon sites appear to be normal to the bathymetry; however, they are aligned with the canyon axis, as is evident in the mean profiles.

The time-series plots of the low-pass filtered currents show the variability of the flow with time and season. Although near-bottom flow tends to be upcoast on each shelf, this is not exclusively true, as is exemplified at the Shelf Break site, where the entire water column can flow downcoast for weeks (fig. 13). At the deeper sites (Slope and Deep Canyon), this upcoast flow is constrained to the middle of the water column and can be transient (figs. 18 and 24). These observations could indicate the presence of the Davidson Undercurrent (or California Counter-current), although more analysis is required to confirm this possibility.

Tidal Parameters

A harmonic tidal analysis was performed on the current-meter data at each site as another measure to determine quality of data. This was accomplished with the t_tide package in Matlab (Pawlowicz, and others, 2002), which is based on the original routines of Foreman (1978). A tidal analysis on vector current data provides ellipse parameters of each constituent used in the analysis (major-and minor-axis amplitude and inclination of major axis with respect to north), as well as a vector tide fit to the data reconstructed from each constituent. The four major constituents for this region are the M_2 and S_2 in the semidiurnal band, and the O_1 and K_1 in the diurnal band (Noble and Xu, 2004). Vertical profiles of the major axis amplitude and inclination of the tidal ellipses for these four constituents at each USGS and OCSD site are plotted in figures 40–48.

Tidal parameters on the San Pedro Shelf from the OCSD moorings (figs. 45–48) are consistent with results from previous measurement programs on this shelf (Noble and Xu, 2004) and other sections of the California Continental Shelf (Rosenberger and others, 2011). Amplification of the M_2 tide toward the bottom is observed at sites near the shelf break (M18 and M21, figs. 45 and 48) and the mid-shelf (M19, fig. 46). Orientation of the M_2 tidal ellipses shift from alongshelf near the surface to cross-shelf near the bottom. Noble and Xu (2004) show that this is due to the internal tide propogating onto the shelf from offshore. This amplification and rotation near the bottom is not observed on the Newport Shelf and Slope, (figs. 40–42), suggesting that the internal tides are not as strong in this region. Both canyon moorings show significant amplification of the M_2 tide near the bottom (figs. 43 and 44) . This phenomenon occurs below the canyon rim at each location, and thus it is not clear if this is due to internal tides or simply a funnelling of the barotropic tide along the canyon.

The tidal ellipses for each constituent can also be plotted on a map of the region to elucidate the eccentricity (ratio of major axis to minor axis) and orientation of the ellipses at differernt depths, with respect to the topography of the region. Figure 49 shows the tidal ellipses from the M2 constituent at several depth levels in the water column at each site. Rather than plot each constituent separately, figure 50 shows the results of a principal components analysis on the combined vector tide fit, with the the variance ellipses plotted.

The eccentricity of the M_2 tidal ellipses (major-axis amplitude/minor-axis amplitude) illustrate how focused the energy is in a particular direction (fig. 49). For instance, the near-bottom tidal currents in the canyon are very focused in the along-canyon direction. Similarly, the near-bottom and mid-depth tidal currents are highly focused alongshore at the Inner Shelf and Shelf Break sites. In contrast, the near-bottom currents near the shelf break at M18 are highly focused cross-shore, demonstrating the importance of the internal tide at this site. Site M21 shows strong M_2 tidal currents near the bottom as well, although not as focused as at M18. Near-bottom tides decrease with magnitude and rotate alongshelf as one moves inshore to site M20 in 19 m water depth.

Conclusions

Six months of data on water-column current speed and direction were obtained by the USGS at five sites in water depths ranging from 15 to 390 m off the coast of southern California in 2011–12. The data were processed using standard quality-assurance/quality-control procedures to ensure completeness and quality. These data will provide invaluable insights to the overall flow patterns in a region of complex bathymetry. These data will also allow for investigations on the interaction between offshore and inshore flow and understanding how these flow patterns influence the transport of sediments and pollutants in the coastal ocean.

Initial results show differences in internal tidal energy between the San Pedro Shelf and the Newport Shelf, as well as variability in this energy between seasons. Future investigations will attempt to elucidate the processes responsible for these differences. The variability of internal tides on continental shelves is not well understood. The full water-column profiles at the Slope and Deep Canyon site suggest the presence of the Davidson Undercurrent and provide a unique opportunity to study how the undercurrent may influence the propogation of internal tides onto the Continental Shelf.

References Cited

Foreman, M.G.G, 1977, Manual for tidal height analysis and prediction: Sidney, British Columbia, Institute of Ocean Sciences Technical Report, Pacific Marine Science Report 77–10.

Foreman, M.G.G., 1978, Manual for tidal current analysis and prediction: Sidney, British Columbia, Institute of Ocean Sciences Technical Report, Pacific Marine Science Report 78–6.

National Oceanic and Atmospheric Administration, Pacific Marine Environmental Laboratory, EPIC netCDF General Conventions, http://www.epic.noaa.gov/epic/document/convention.htm.

National Oceanic and Atmospheric Administration, National Data Buoy Center database, http://www.ndbc.noaa.gov.

National Oceanic and Atmospheric Administration, National Ocean Service, Center for Operational Oceanographic Products and Services, http://co-ops.nos.noaa.gov.

Noble, M.A and Xu, J.P., 2004, Huntington Beach Shoreline contamination investigation, phase III: U.S. Geological Survey Open File Report 2004–1019.

Noble, M. A., Rosenberger, K.J., Hamilton, P., and Xu, J.P., 2009, Coastal ocean transport patterns in the central Southern California Bight, *in* Lee, H.J., and Normark, W.R., eds., Earth science in the urban ocean: The Southern California continental borderland: Boulder, Colo., The Geological Society, Special Paper 454, p. 193–226.

Hamilton, P., Noble, M.A, Largier, J., Rosenfeld, L.K., and Robertson, G., 2006, Cross-shelf subtidal variability in San Pedro Bay during summer, 2001: Continental Shelf Research, v. 208, p. 681–702.

IEEE, 1980, 1978 practical salinity scale equations: Institute of Electrical and Electronics Engineers Journal of Oceanic Engineering, OE-5, no. 1, 14 p.

Pawlowicz, P., Beardsley, B., and Lentz, S., 2002, Classical tidal harmonic analysis including error estimates in MATLAB using T_TIDE: Computers and Geosciences, v. 28, p. 929–937.

Rosenberger, K.J., Noble, M.A., Sherwood, C.R., Martini, M.M., Ferreira, J.T., and Montgomery, Ellyn, 2011, Palos Verdes Shelf oceanographic study; data report for observations December 2007–April 2008: U.S. Geological Survey Open-File Report 2010–1240, 118 p., http://pubs.usgs.gov/of/2010/1240/.

Science Applications International Corporation (SAIC), 2009, Orange County Sanitation District ocean current studies: Analysis of inter- and intra-annual variability in coastal currents: San Diego, California, prepared by Science Applications International Corporation for Orange County Sanitation District, SAIC Report, 62 p.

U.S. Geological Survey, 2001, National Water Information System (NWISWeb): U.S. Geological Survey database, available at http://waterdata.usgs.gov/nwis/.

University Corporation for Atmospheric Research, Unidata Program Center, 2013, NetCDF Users Guide, https://www.unidata.ucar.edu/software/netcdf/docs/user_guide.html.

Weather Underground, 1995, Personal Weather Station database, http://classic.wunderground.com.

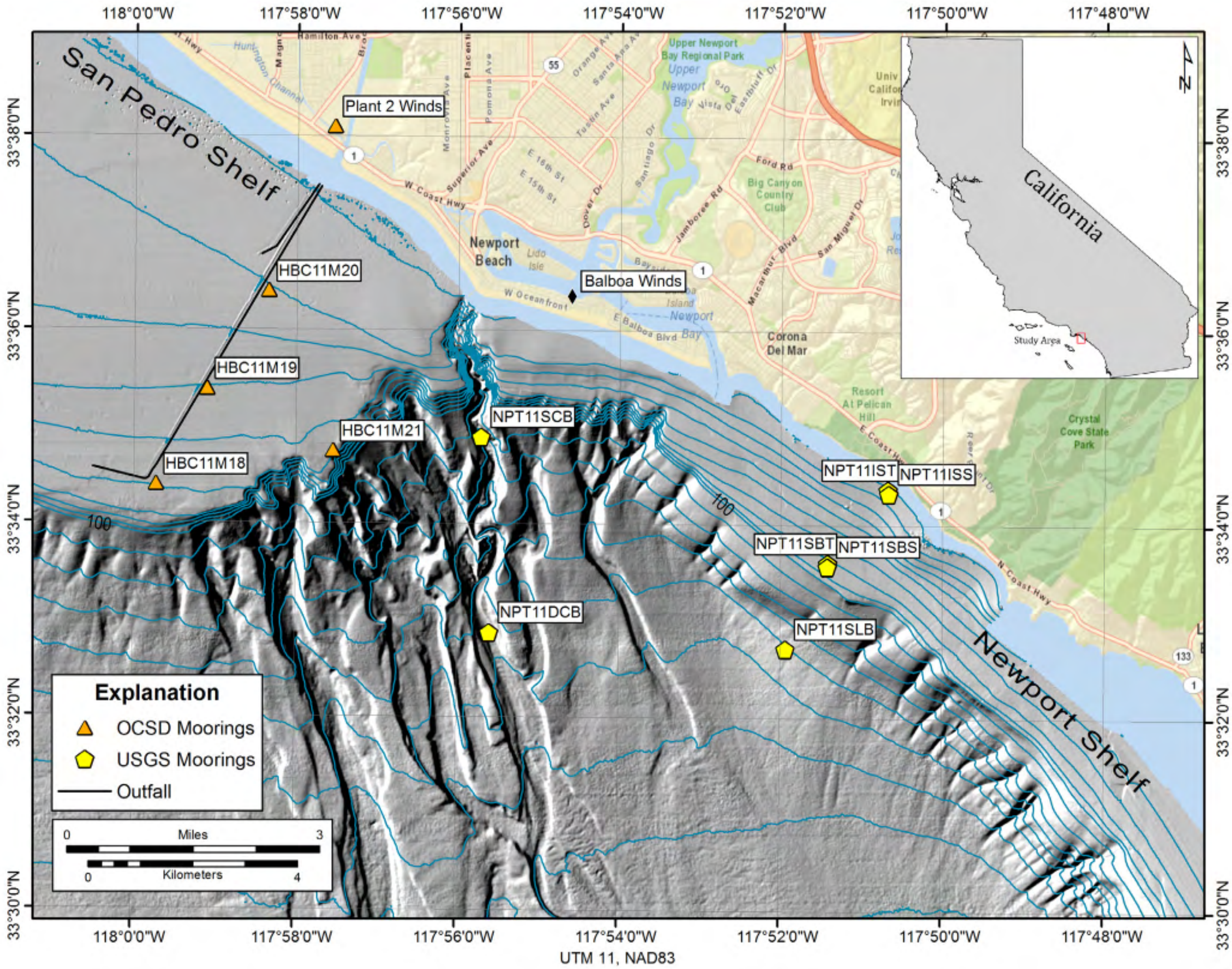

Figure 1. Map of study area showing Orange County Sanitation District and U.S. Geological Survey moorings in the Newport Shelf program and their locations relative to the San Pedro Shelf, Newport Beach, California. Contours are plotted every 10 m from 0 to 100 m depth, and every 50 m deeper than 100 m.

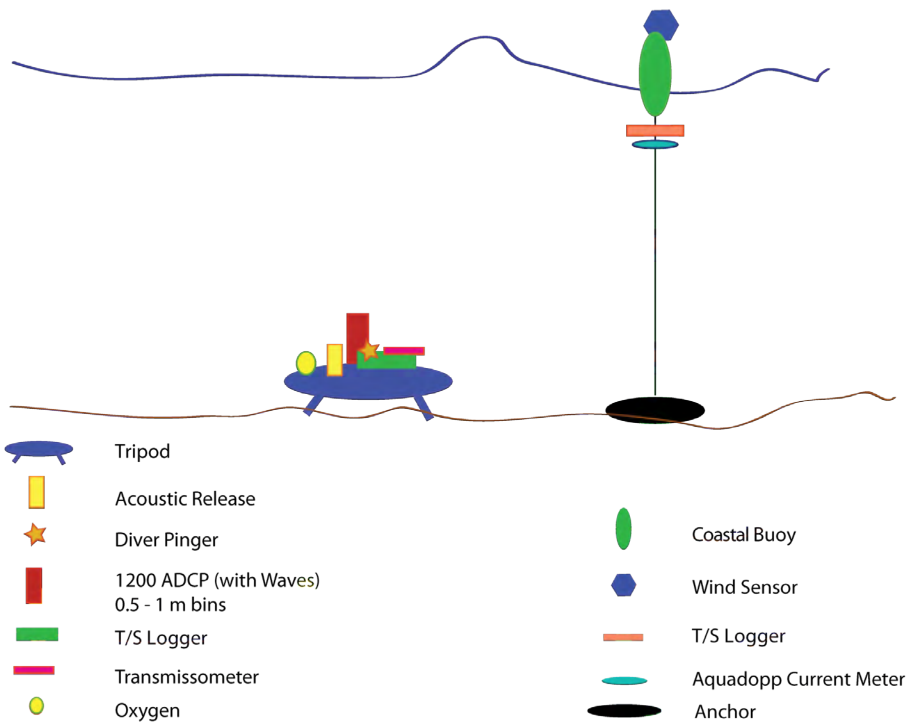

Figure 2. Diagram of the mooring and tripod placed on the inner shelf of the Newport Shelf (Inner Shelf site), Newport Beach, California. Mooring depth, 14 m.

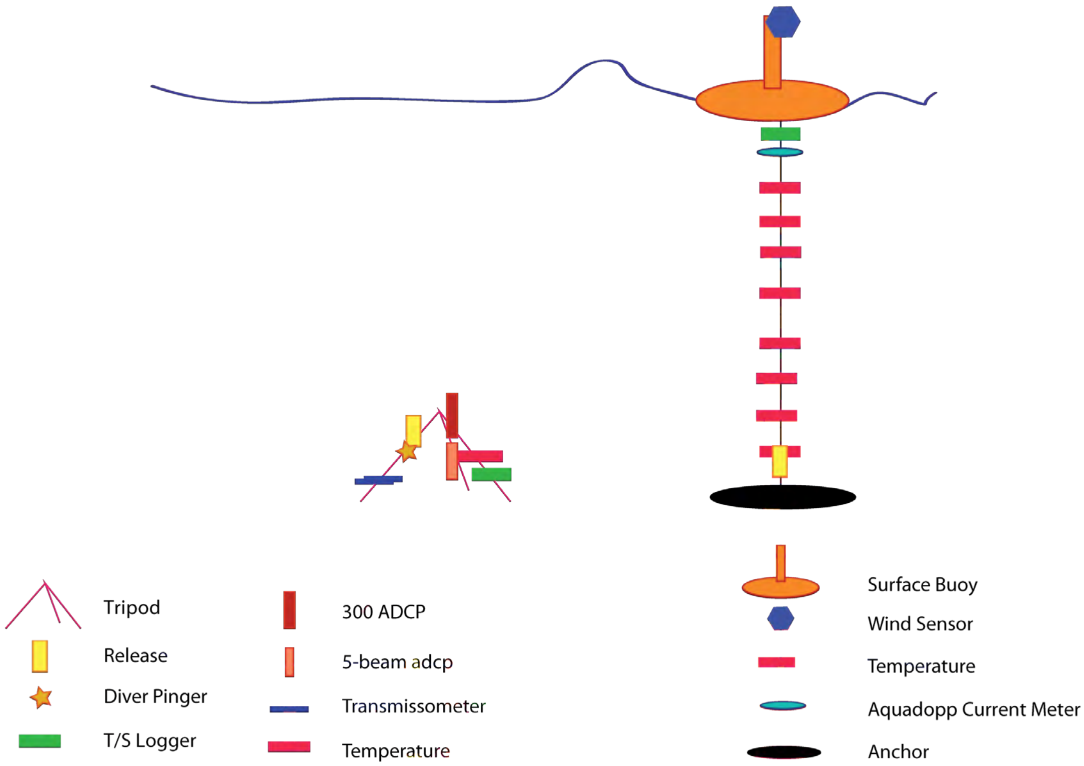

Figure 3. Diagram of the mooring and tripod placed on the shelf break of the Newport Shelf (Shelf Break site), Newport Beach, California. Mooring depth, 85 m.

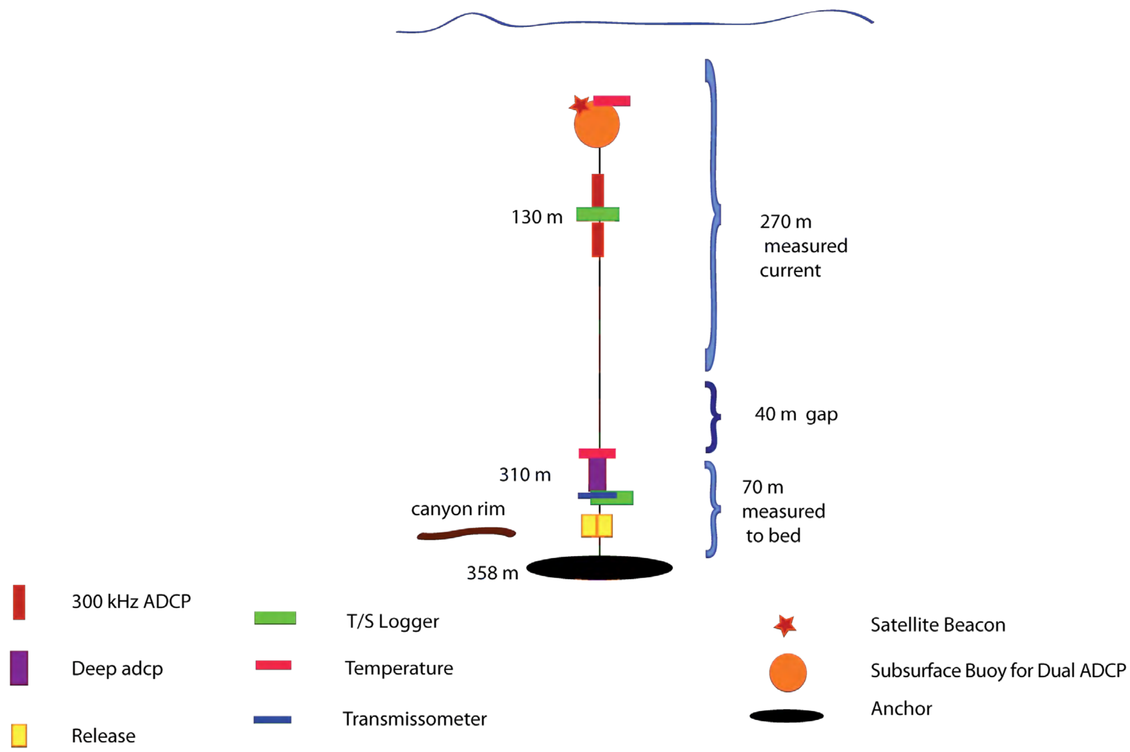

Figure 4. Diagram of mooring placed on the slope off the Newport Shelf (Slope site), Newport Beach, California. Mooring depth, 358 m.

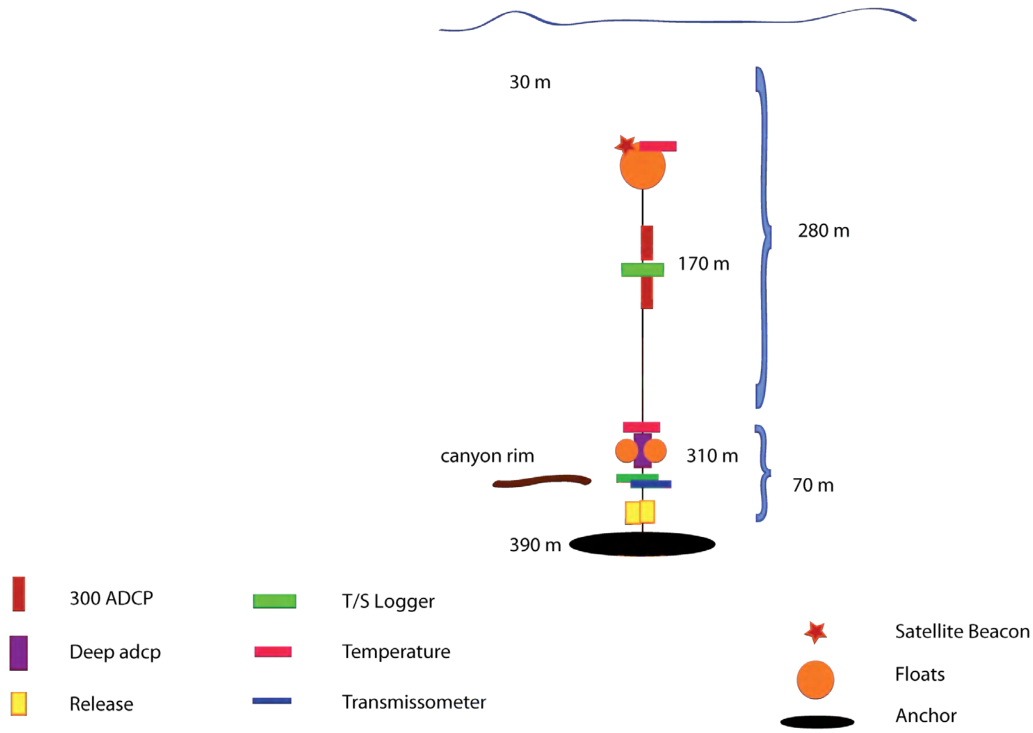

Figure 5. Diagram of mooring placed in the deep section of Newport Canyon (Deep Canyon site), Newport Beach, California. Mooring depth, 380 m.

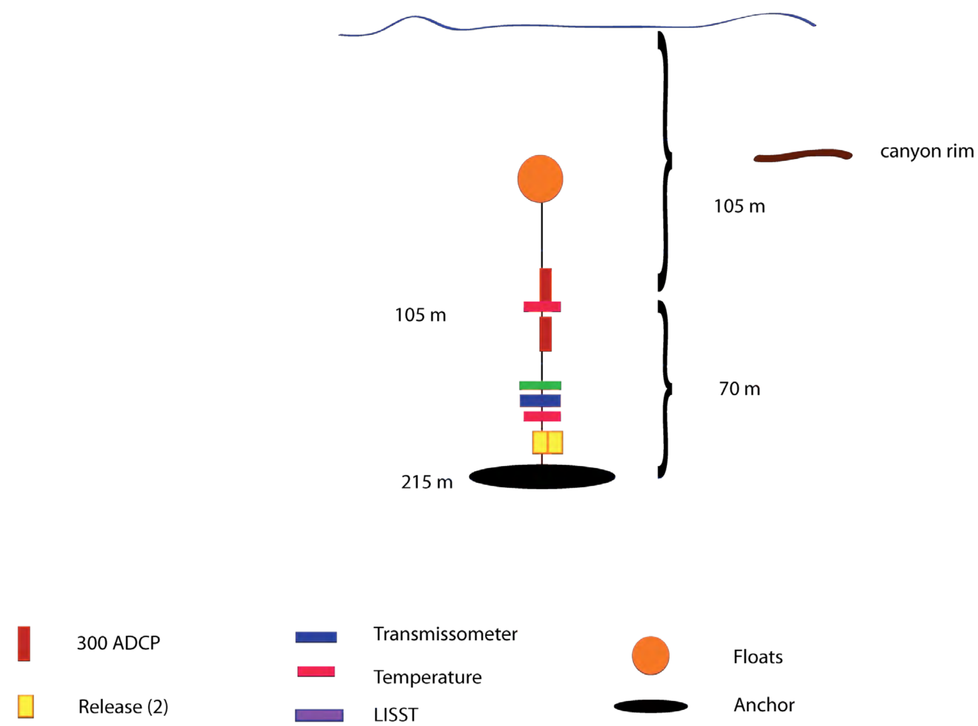

Figure 6. Diagram of mooring placed in the shallow section of Newport Canyon (Shallow Canyon site), Newport Beach, California. Mooring depth, 215 m.

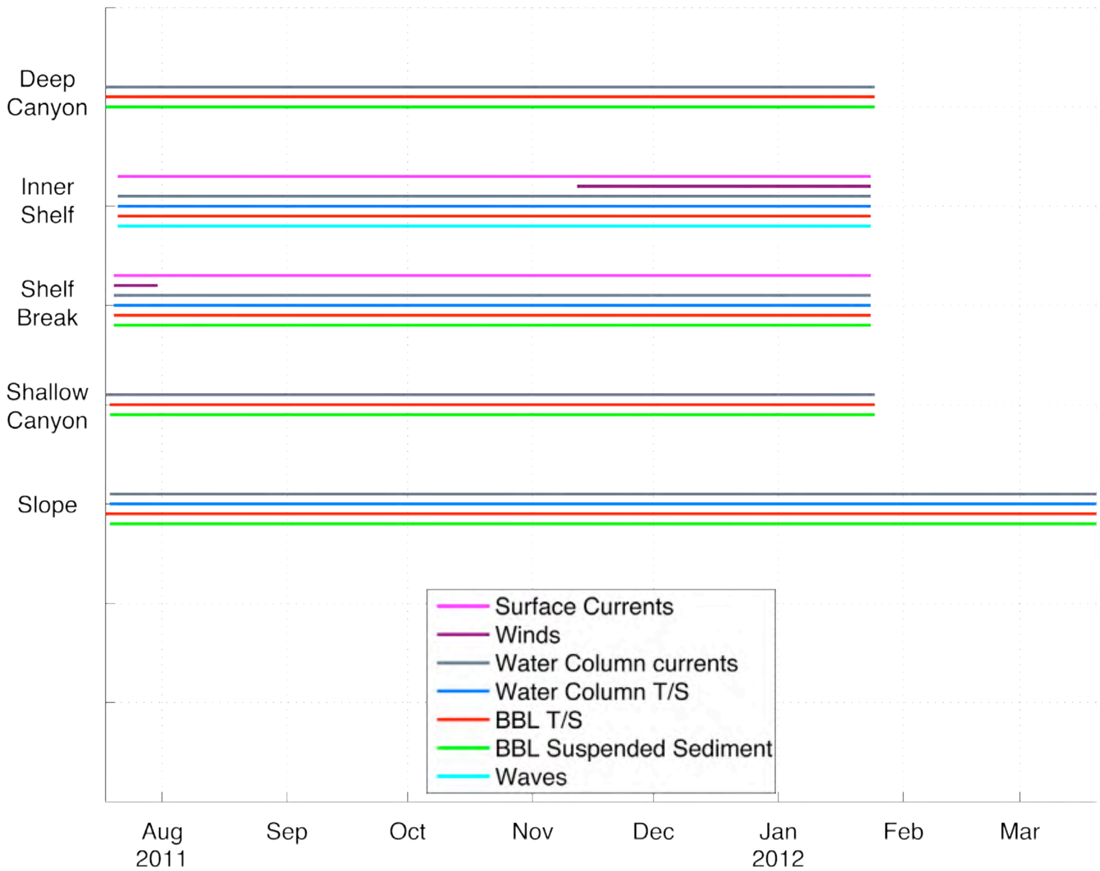

Figure 7. Timeline of data acquired by the U.S. Geological Survey on the Newport Shelf and slope, by platform and data type, Newport Beach, California.

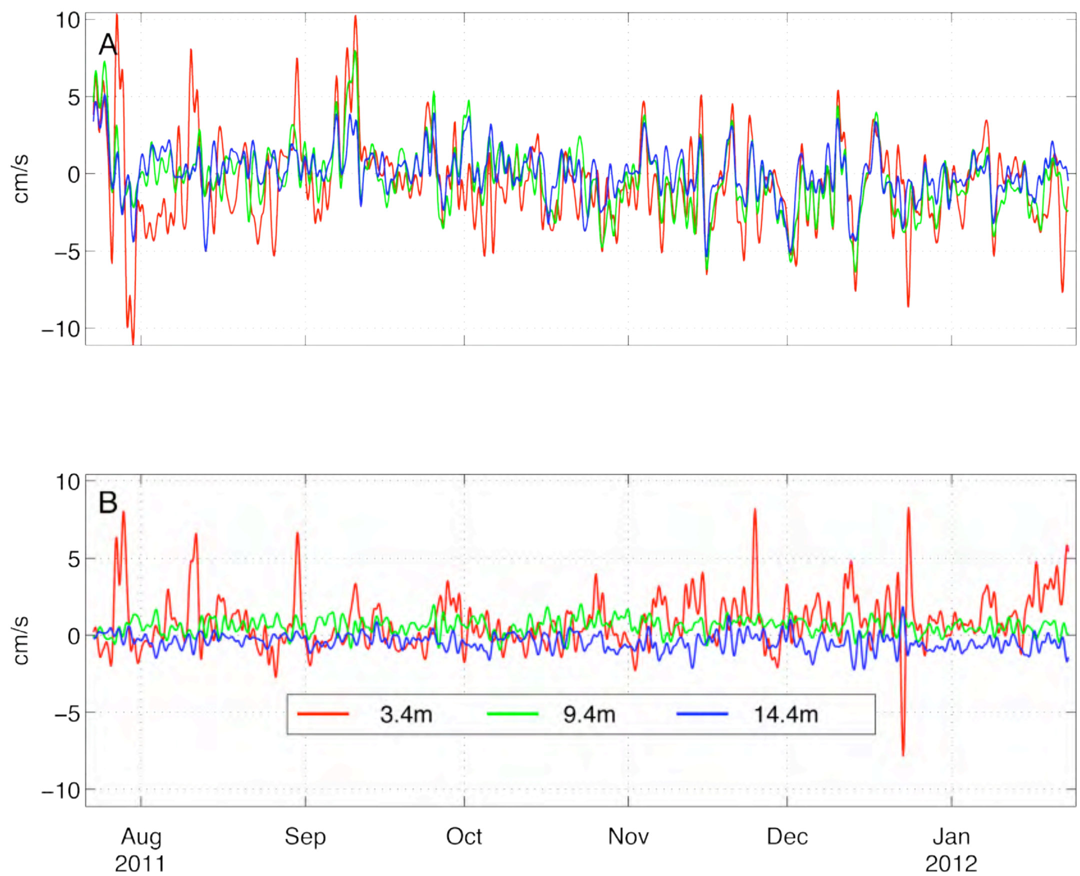

Figure 8. Low-pass filtered currents measured at several depth levels in the water column at the Inner Shelf site, Newport Beach, California. *A*, Alongshore currents. *B*, Cross-shore currents. The alongshore direction is determined using a depth-averaged value of major axis inclination from a principal components analysis of the current-meter data from the acoustic Doppler current profilers.

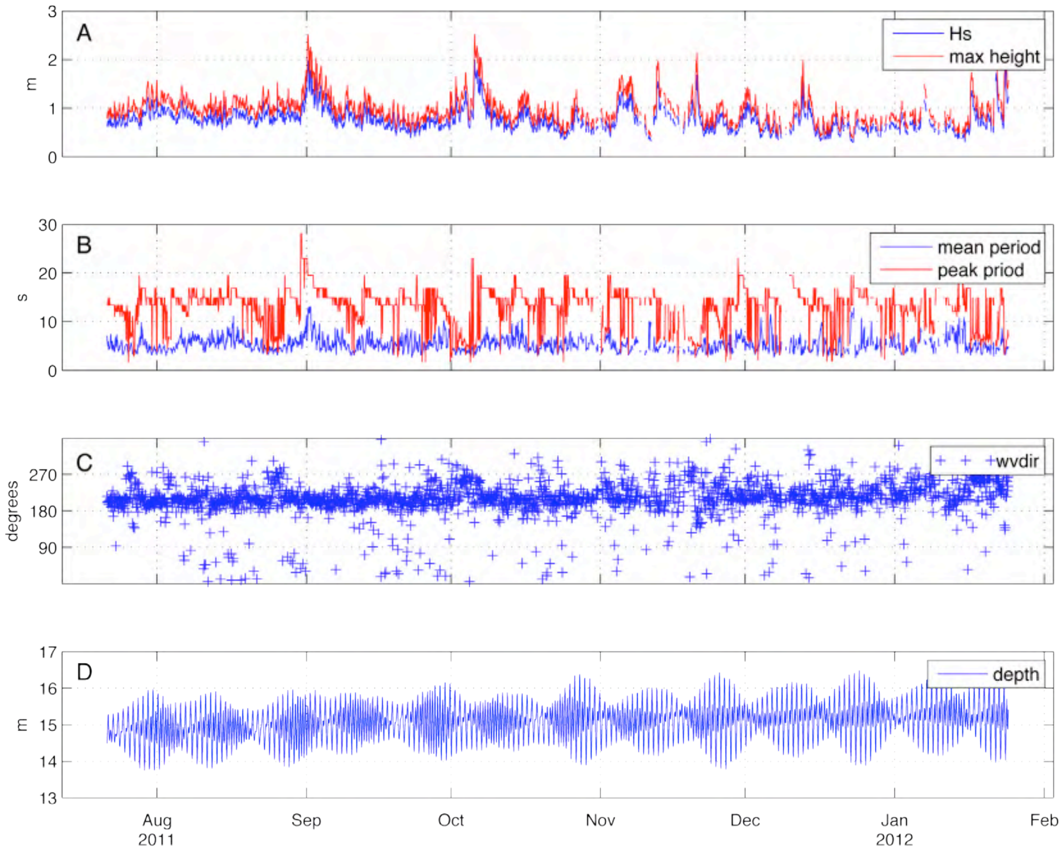

Figure 9. Surface-wave parameters measured by the ADCP on the bottom-mounted tripod at the Inner Shelf site, Newport Beach, California. *A,* Significant wave height and maximum wave height. *B,* Mean wave period and peak wave period. *C*, Mean wave direction. *D,* Water depth.

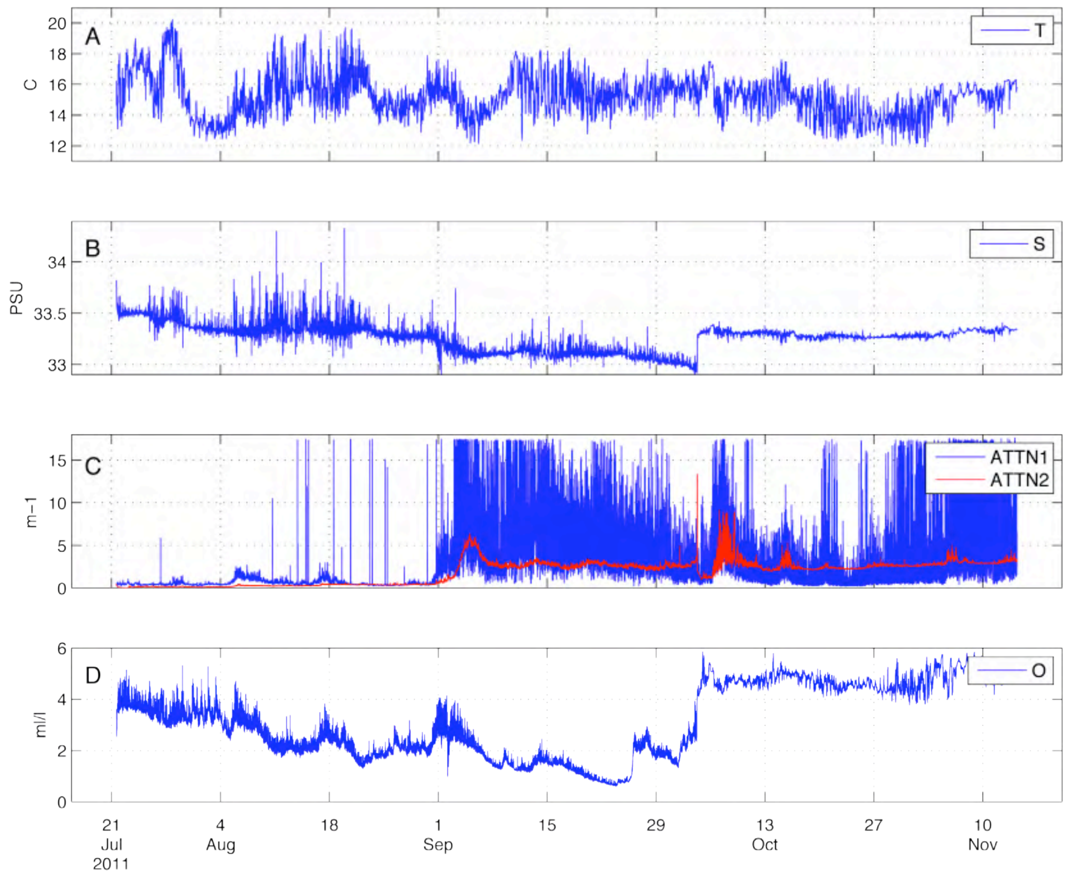

Figure 10. Near-bottom water properties and suspended sediment data at the Inner Shelf site, Newport Beach, California. *A*, Temperature. *B*, Salinity. *C*, Light attenuation. *D*, Dissolved oxygen.

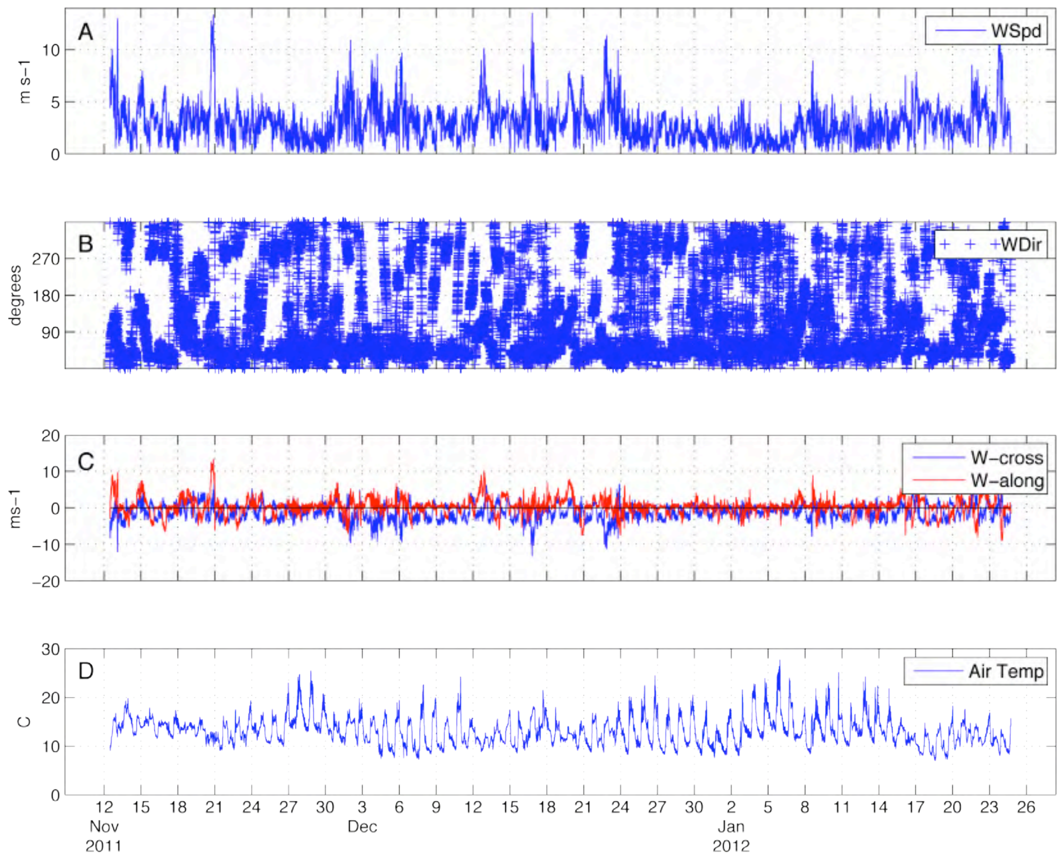

Figure 11. Meteorological parameters at the Inner Shelf site, Newport Beach, California. A, Wind speed. *B*, Wind direction (blowing from). *C*, Vector components of winds (alongshore and cross-shore). *D*, Air temperature.

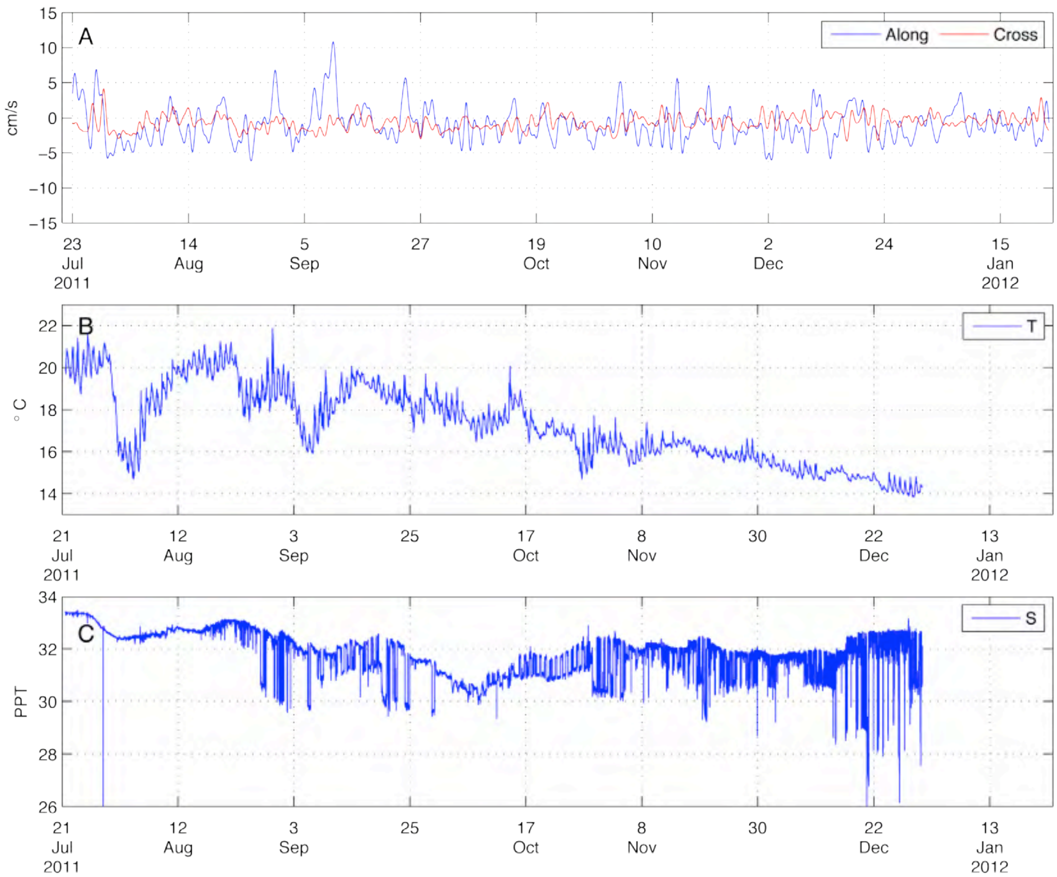

Figure 12. Surface currents and water properties at the Inner Shelf site, Newport Beach, California. *A*, Low-pass filtered alongshore and cross-shore currents. *B*, Water temperature. *C*, Salinity.

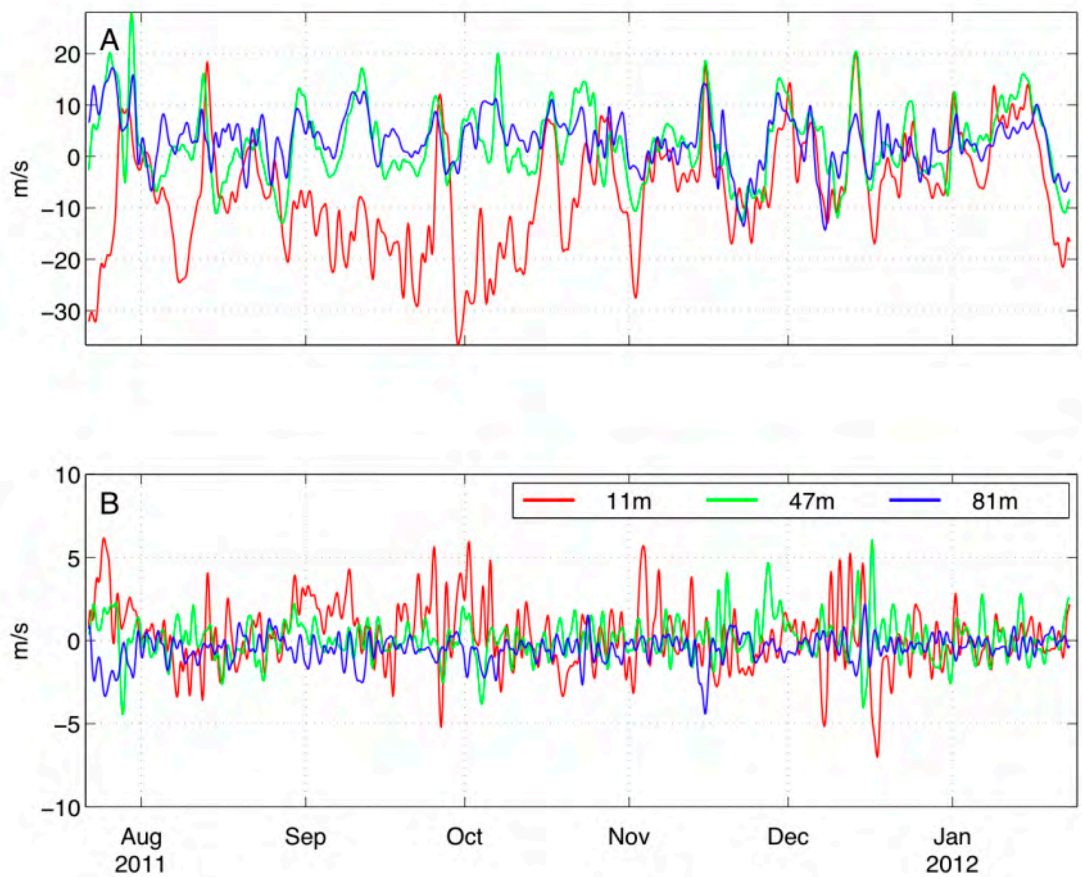

Figure 13. Low-pass filtered currents measured at several depth levels in the water column at the Shelf Break site. *A*, Alongshore currents. *B*, Cross-shore currents. The alongshore direction is determined using a depth-averaged value of major axis inclination from a principal components analysis of the current-meter data from this site.

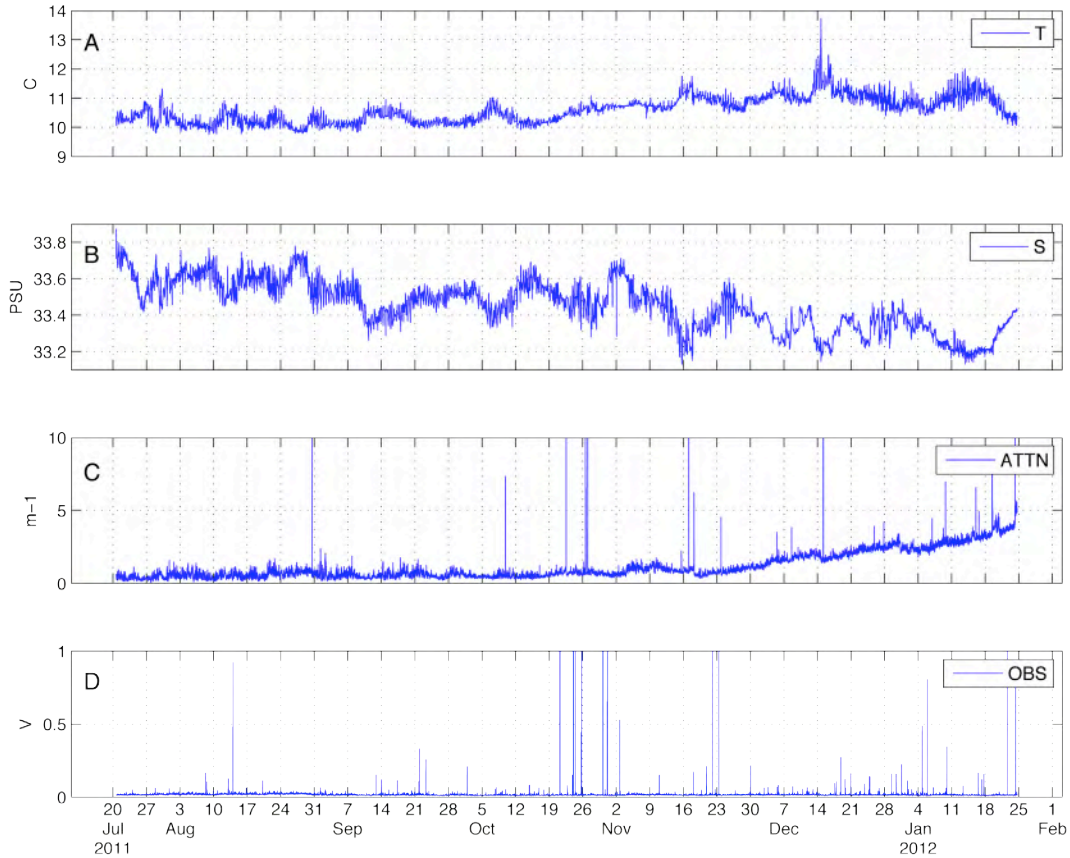

Figure 14. Near-bottom water properties and suspended sediment data at the Shelf Break site, Newport Beach, California. *A*, Temperature. *B*, Salinity. *C*, Light attenuation (third panel). *D*, Optical backscatter.

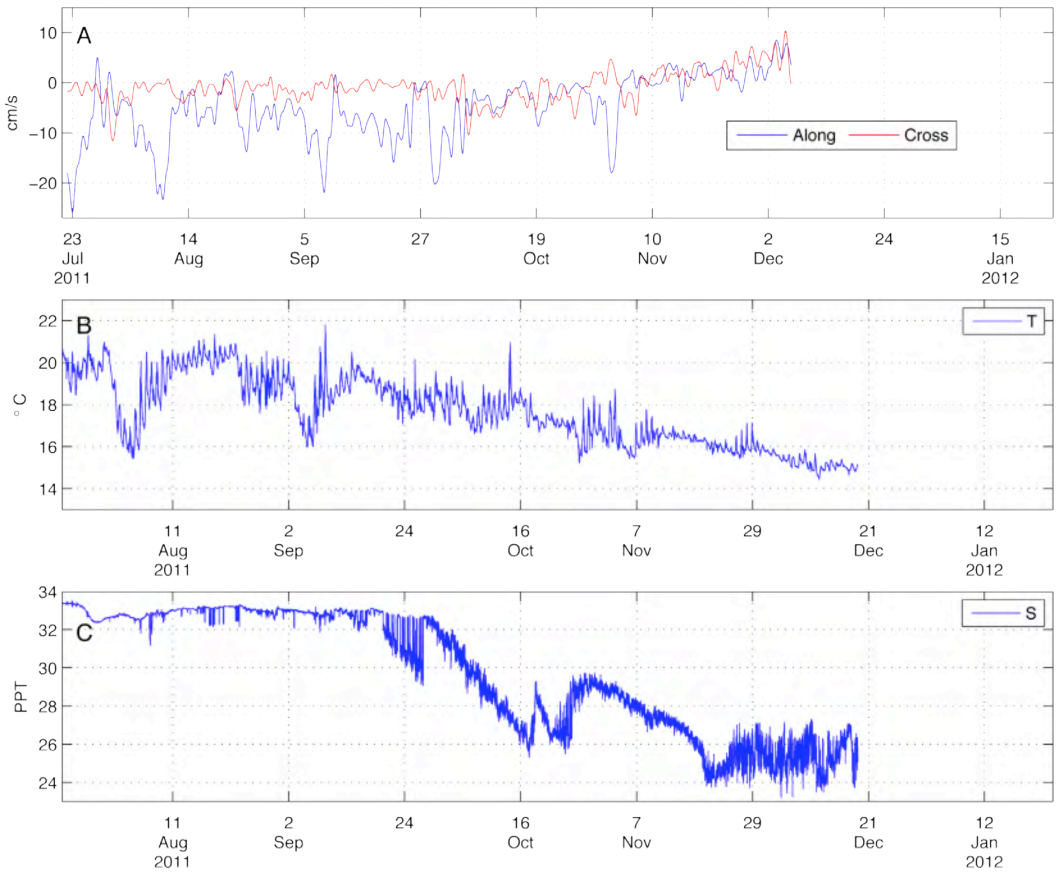

Figure 15. Surface currents and water properties at the Shelf Break site, Newport Beach, California. *A*, Low-pass filtered alongshore and cross-shore currents. *B*, Water temperature. *C*, Salinity.

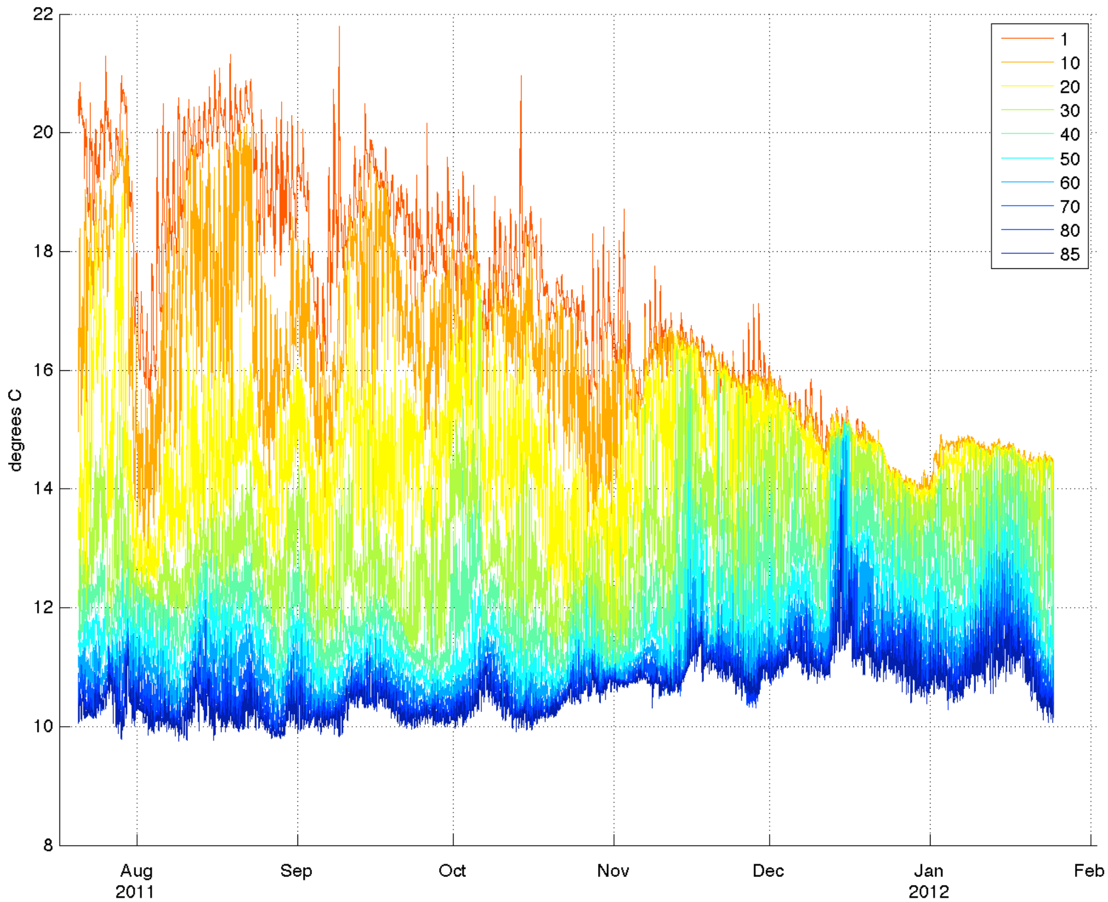

Figure 16. Water-column temperature data at the Shelf Break site, Newport Beach, California.

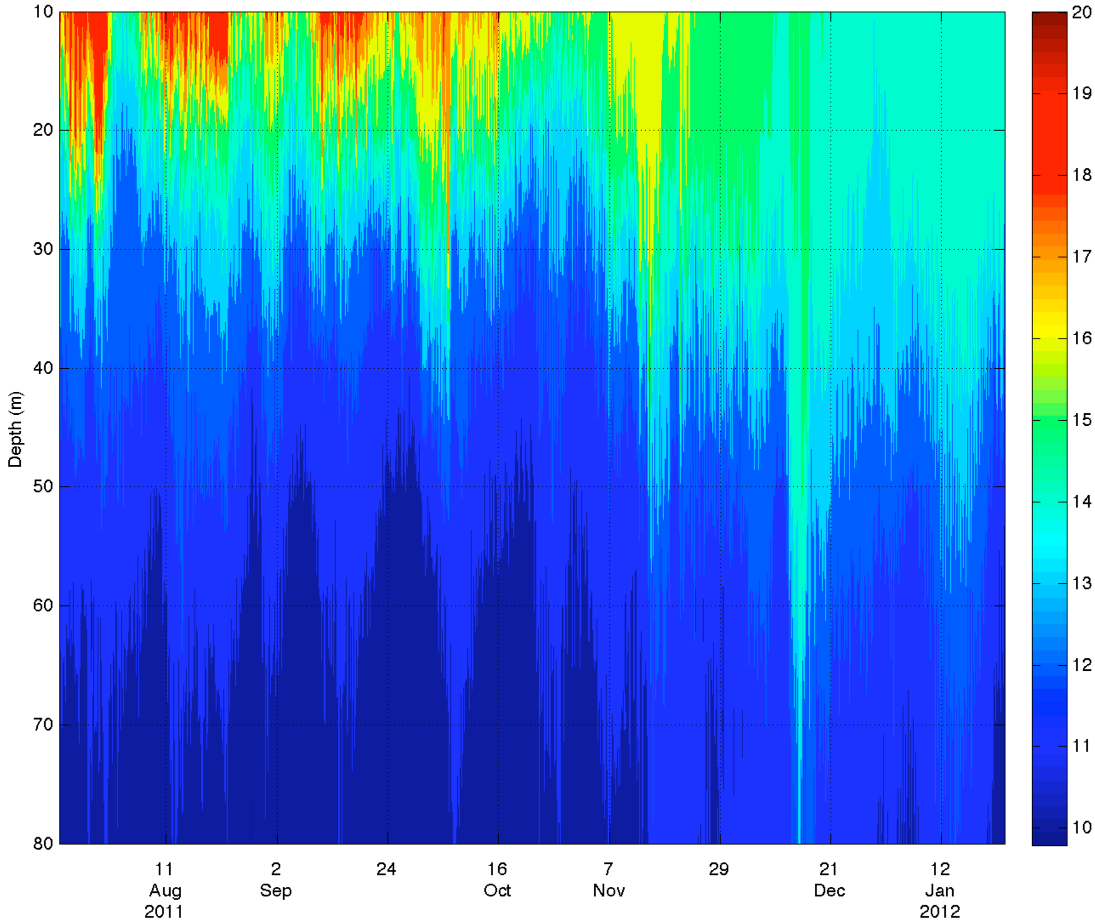

Figure 17. Contours of water-column temperature data at the Shelf Break site, Newport Beach, California.

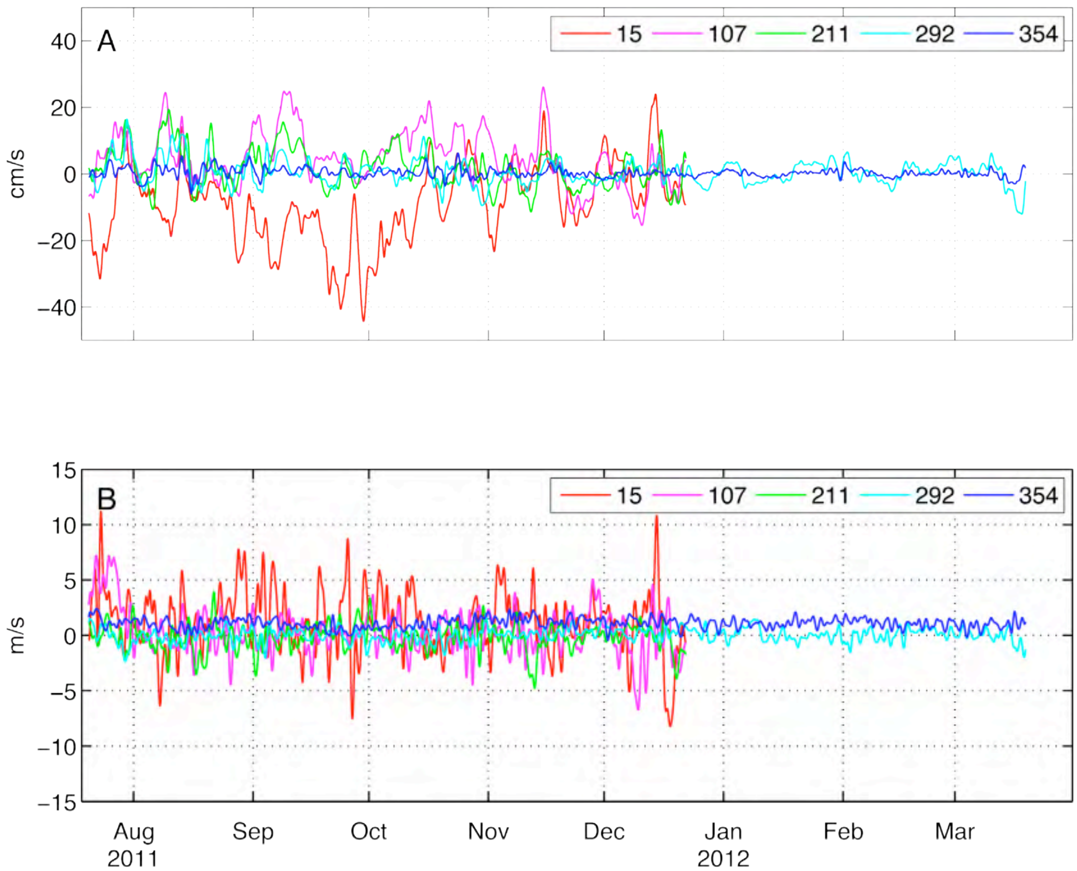

Figure 18. Low-pass filtered currents measured at several depth levels in the water column at the Slope site, Newport Beach, California. *A*, Alongshore and *B*, Cross-shore. The alongshore direction is determined using a depth averaged value of major axis inclination from a principal-components analysis of the current-meter data at this site.

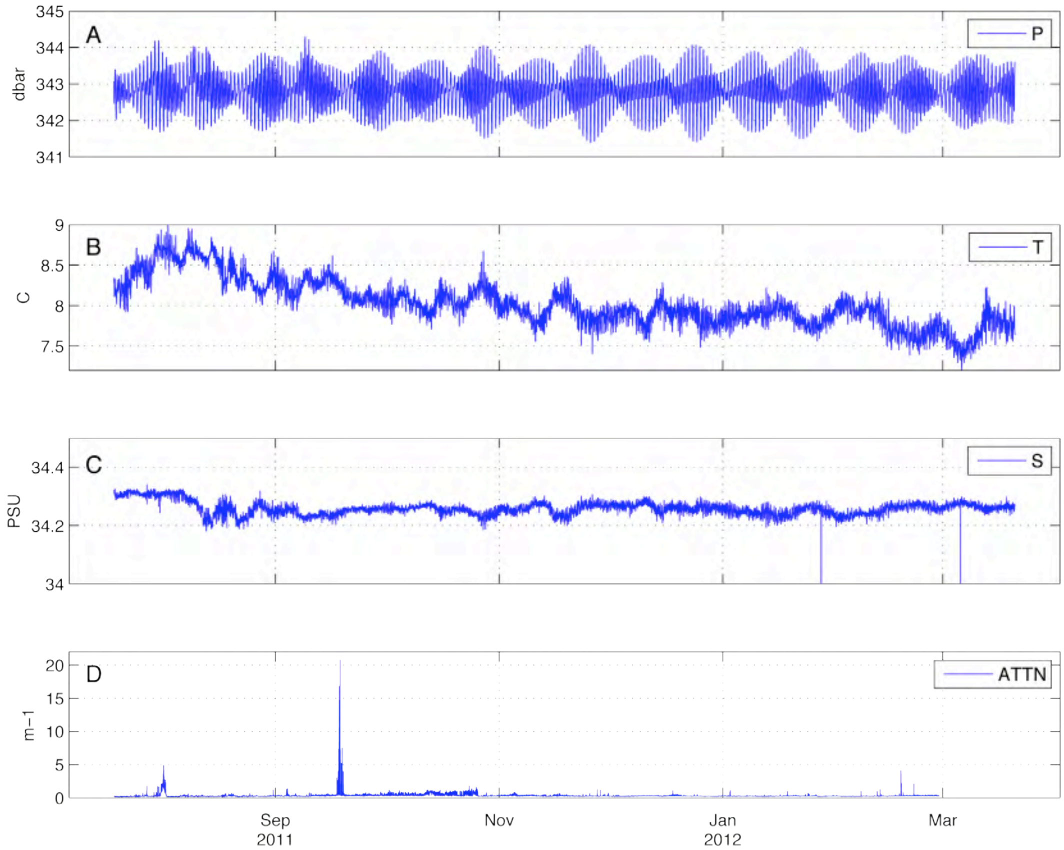

Figure 19. Near-bottom water properties and suspended sediment data at the Slope site, Newport Beach, California. *A*, Pressure. *B*, Temperature. *C*, Salinity. *D*, Light attenuation.

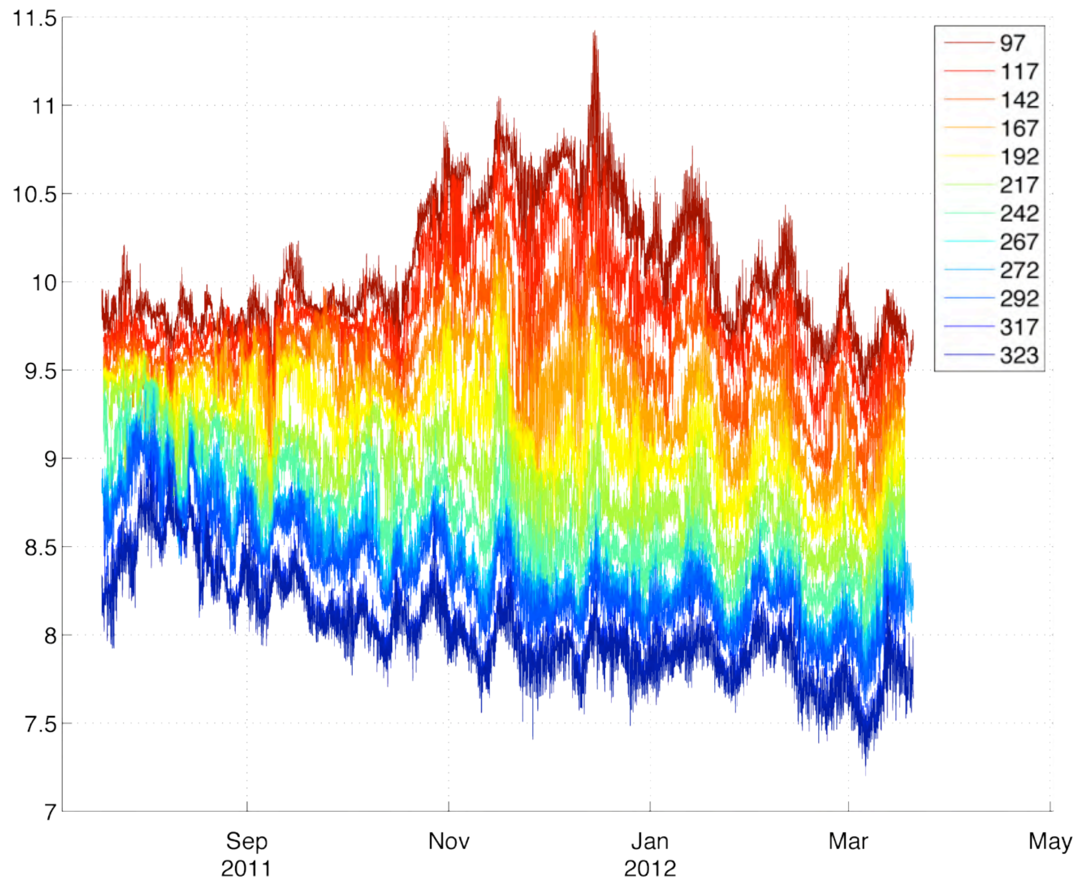

Figure 20. Water-column temperature data at the Slope site, Newport Beach, California.

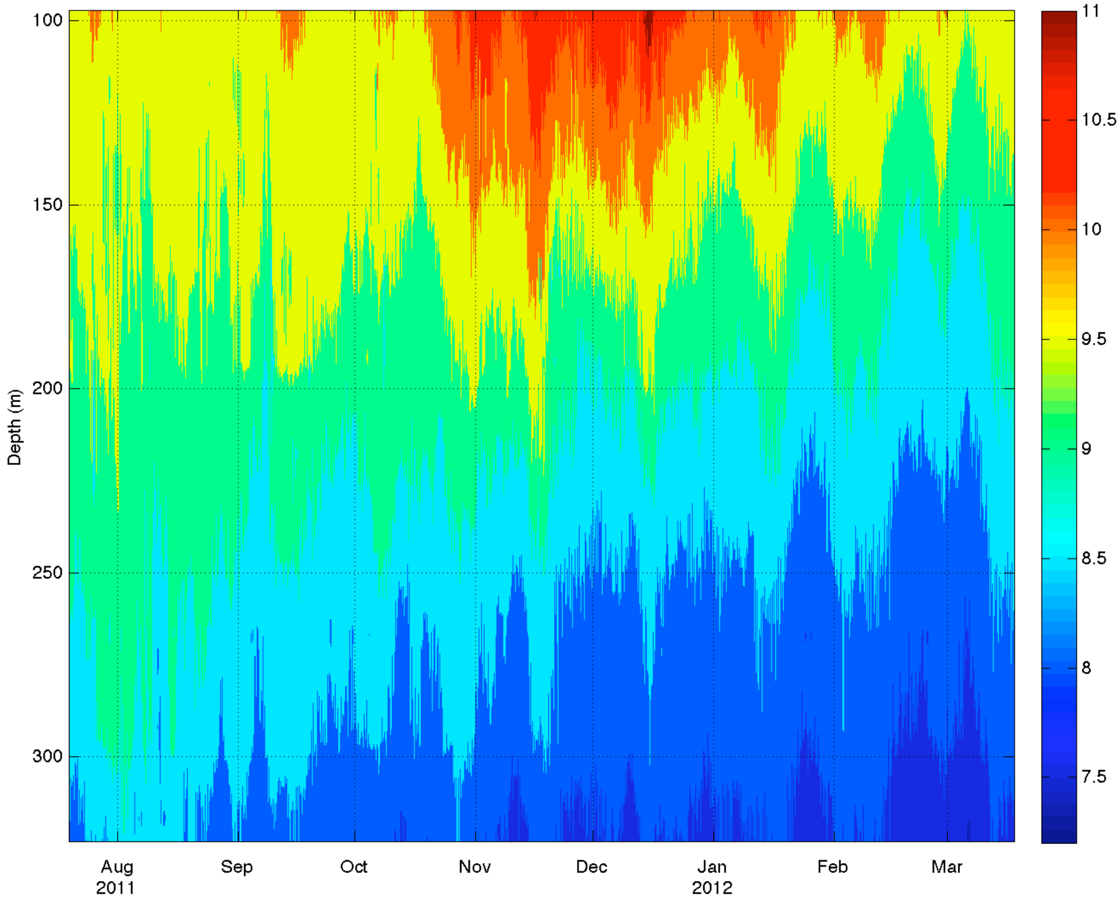

Figure 21. Contours of water-column temperature at the Slope site, Newport Beach, California.

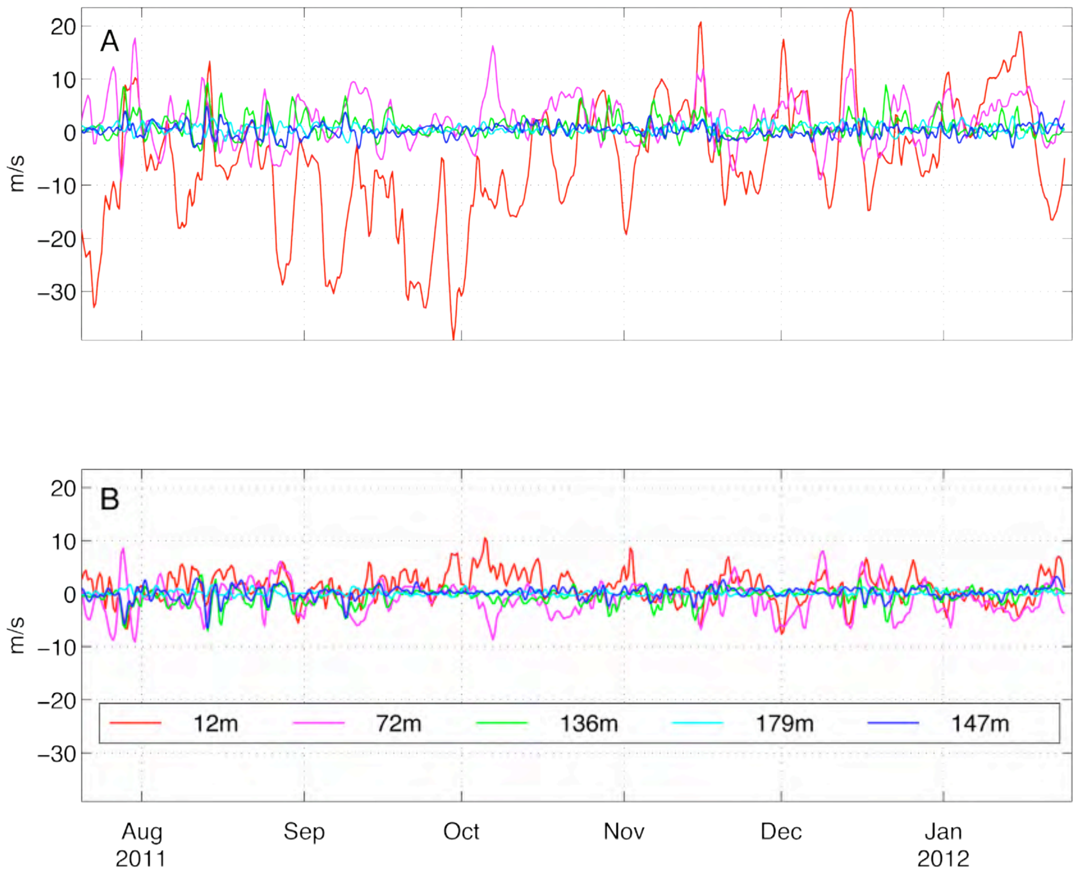

Figure 22. Low-pass filtered currents measured at several depth levels in the water column at the Shallow Canyon site, Newport Beach, California. *A*, Alongshore currents. *B*, Cross-shore currents. The alongshore direction is determined using a depth-averaged value of major axis inclination from a principal components analysis of the current-meter data for a given instrument at this site.

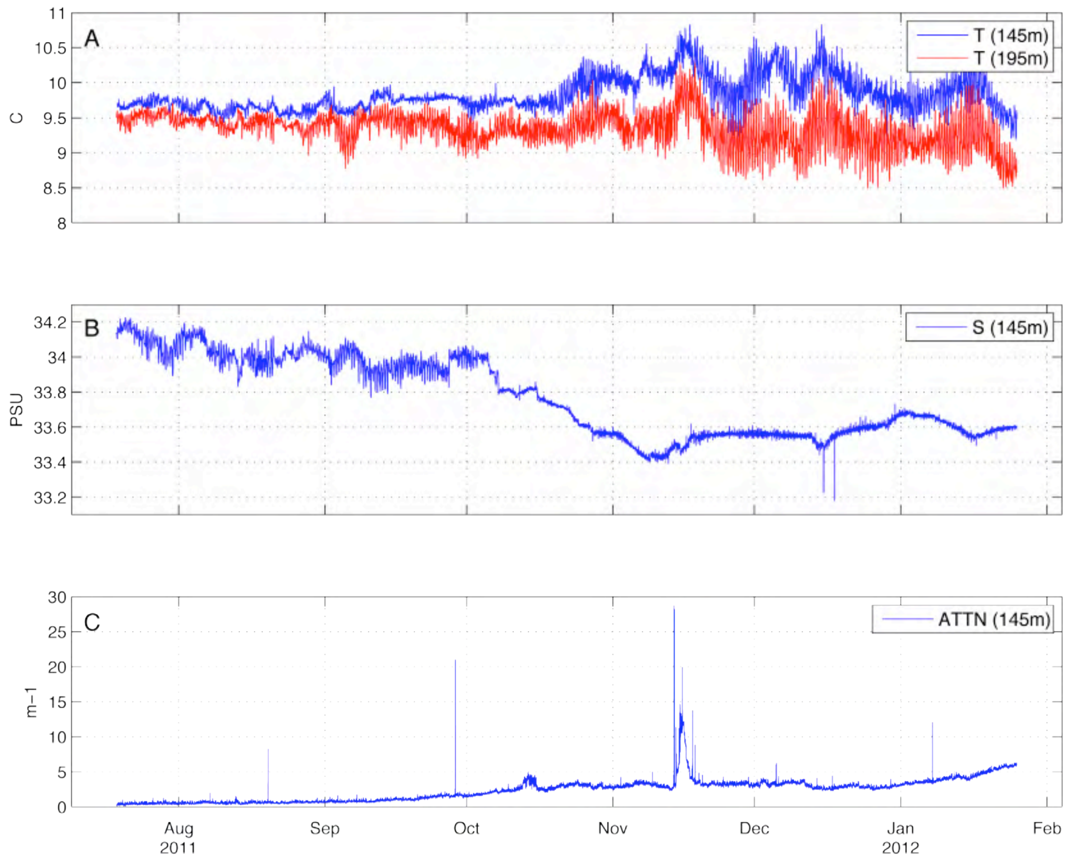

Figure 23. Near-bottom water properties and suspended sediment data at the Shallow Canyon site, Newport Beach, California. *A*, Temperature. *B*, Salinity. *C*, Light attenuation.

Figure 24. Low-pass filtered currents measured at several depth levels in the water column at the Deep Canyon site, Newport Beach, California. *A*, Alongshore. *B*, Cross-shore. The alongshore direction is determined using a depth-averaged value of major axis inclination from a principal components analysis of the current- meter data for a given instrument at this site.

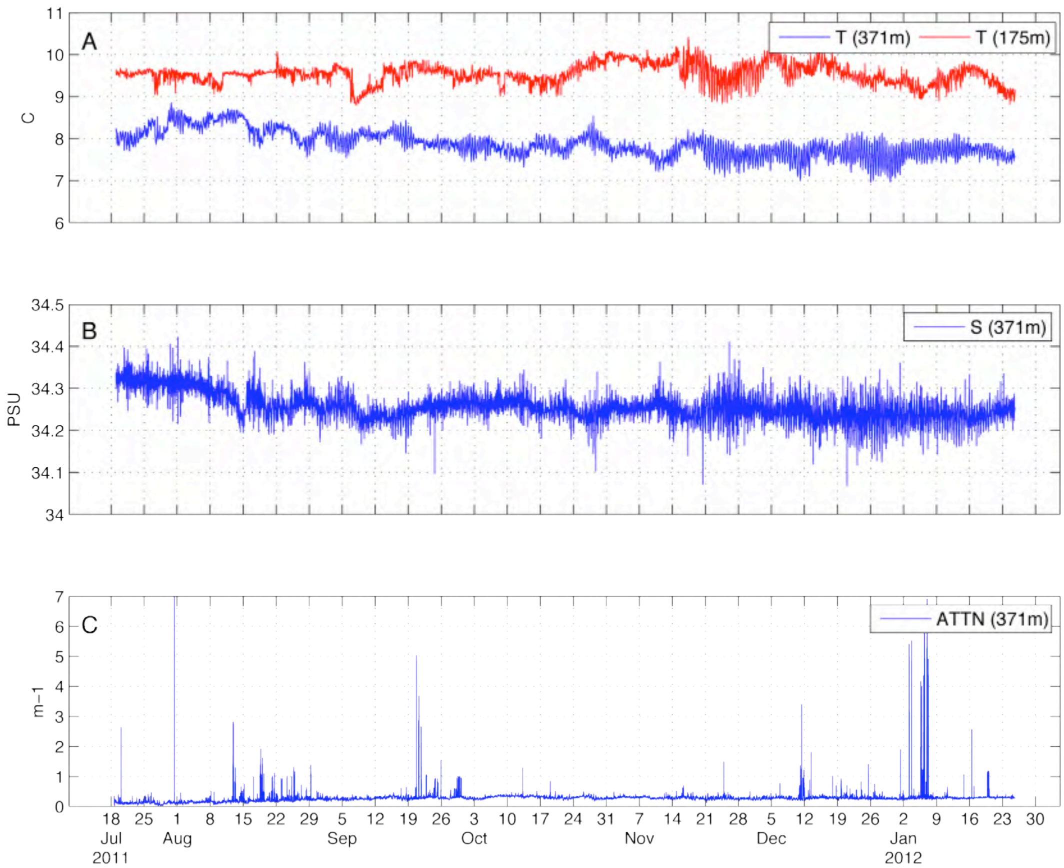

Figure 25. Near-bottom and mid-water column water properties and near-bottom suspended sediment at the Slope site, Newport Beach, California. *A*, Temperature. *B*, Salinity. *C*, Light attenuation.

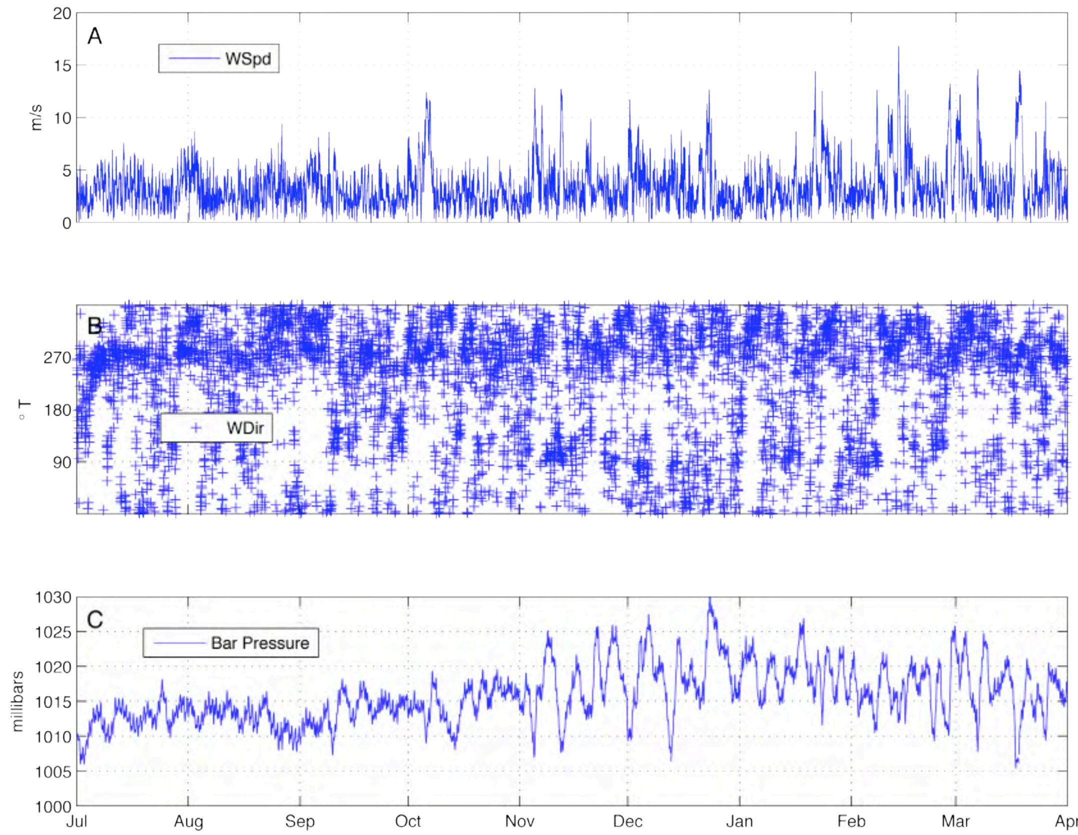

Figure 26. Meteorological parameters measured by the National Oceanic and Atmospheric Administration met-ocean buoy number 46025 in the Santa Monica Basin, 33 nautical miles west-southwest of Santa Monica, California. *A*, Wind speed. *B*, Wind direction (blowing from). *C*, Barometric pressure.

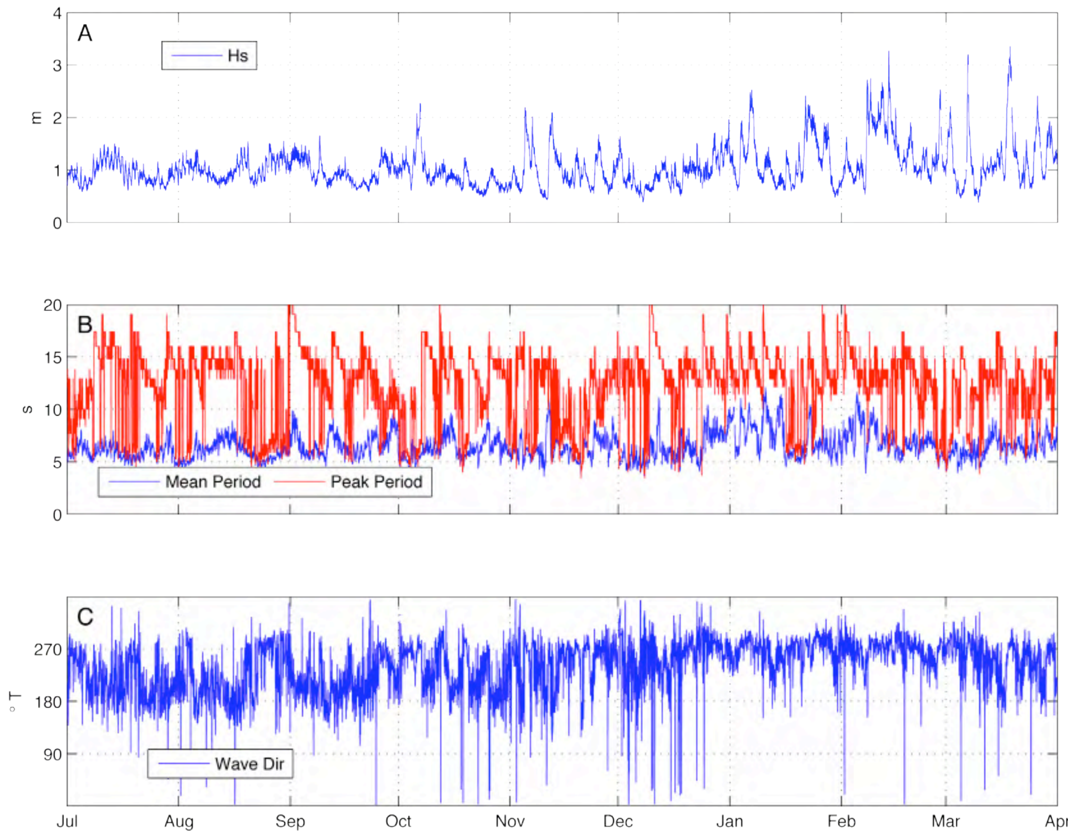

Figure 27. Surface-wave parameters measured by the National Oceanic and Atmospheric Administration met-ocean buoy number 46025 in the Santa Monica Basin, 33 nautical miles west-southwest of Santa Monica, California. *A*, Significant-wave height. *B*, Mean wave period and peak wave period. *C,* Mean wave direction.

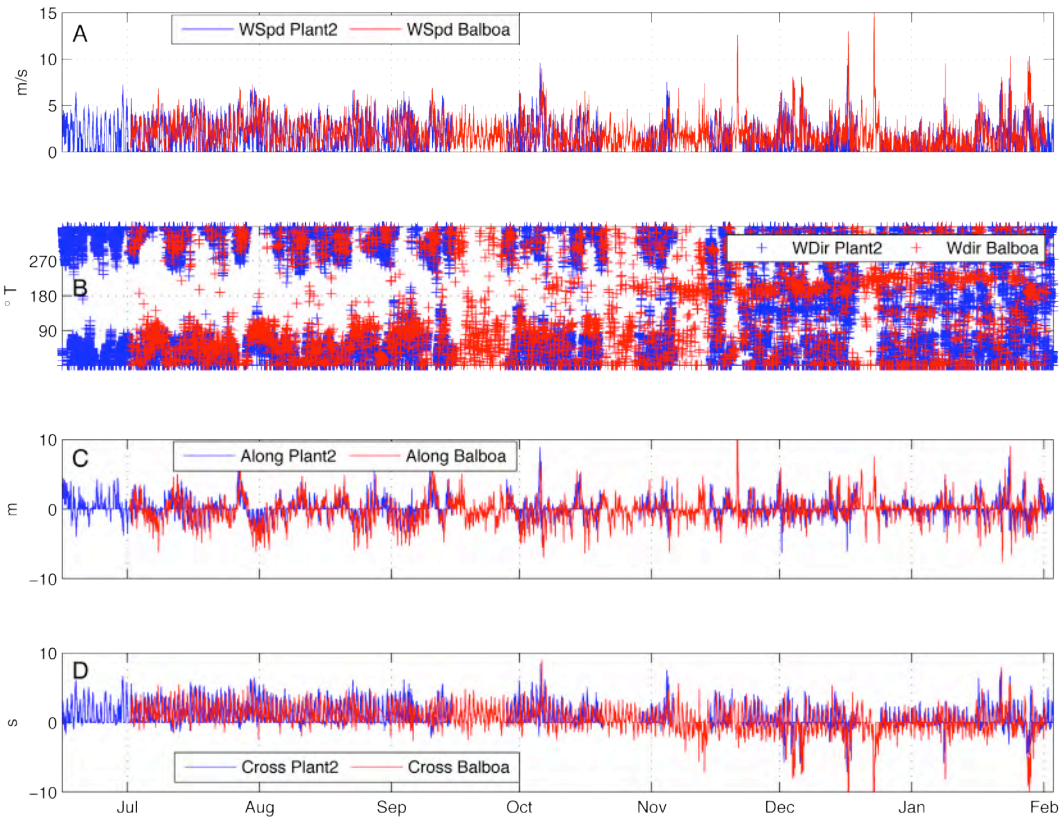

Figure 28. Meteorological parameters measured by the Orange County Sanitation District meteorological station at Plant2 and a personal weather station on the Balboa Peninsula at the entrance to Newport Harbor, Newport Beach, California. *A*, Wind speed. *B*, Wind direction (blowing from). *C*, Alongshore component. *D*, Cross-shore component.

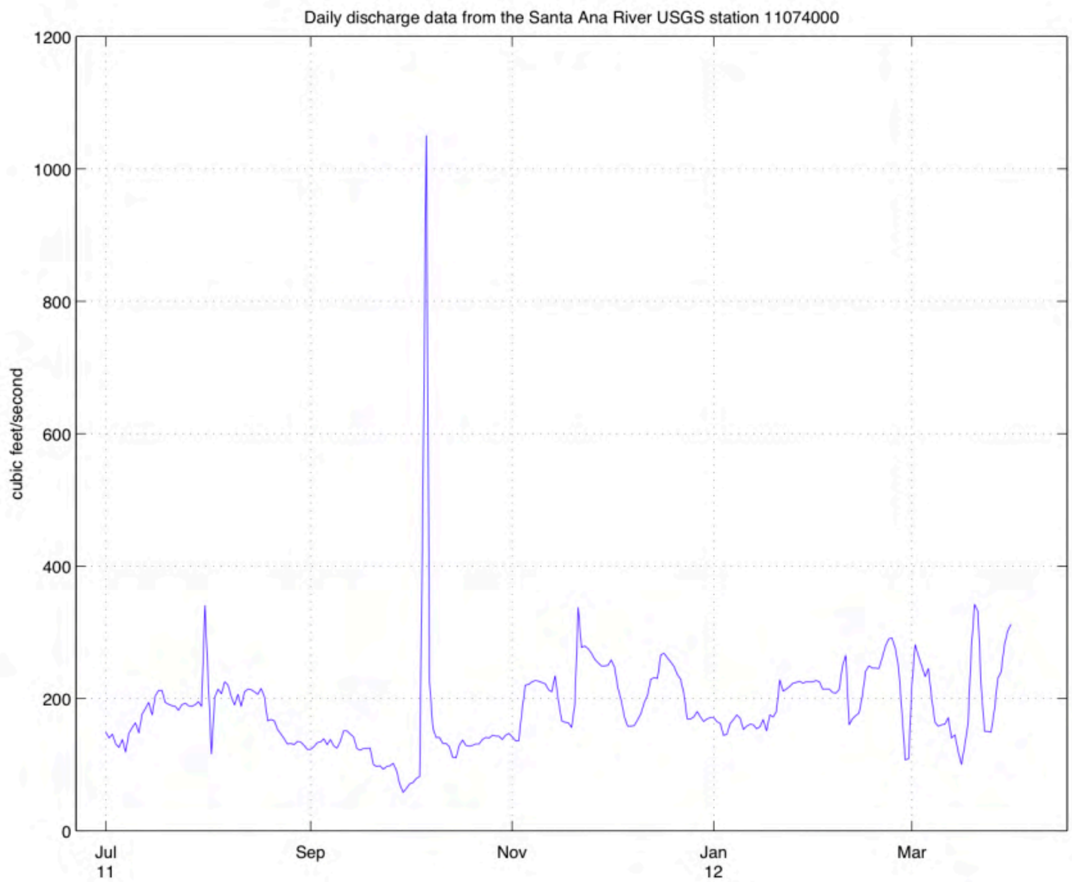

Figure 29. Daily mean river discharge data for the deployment period from the USGS streamflow-gaging station number 11074000 on the Santa Ana River, feeding into Newport Harbor, Newport Beach, California. Discharge is measured in cubic feet per second.

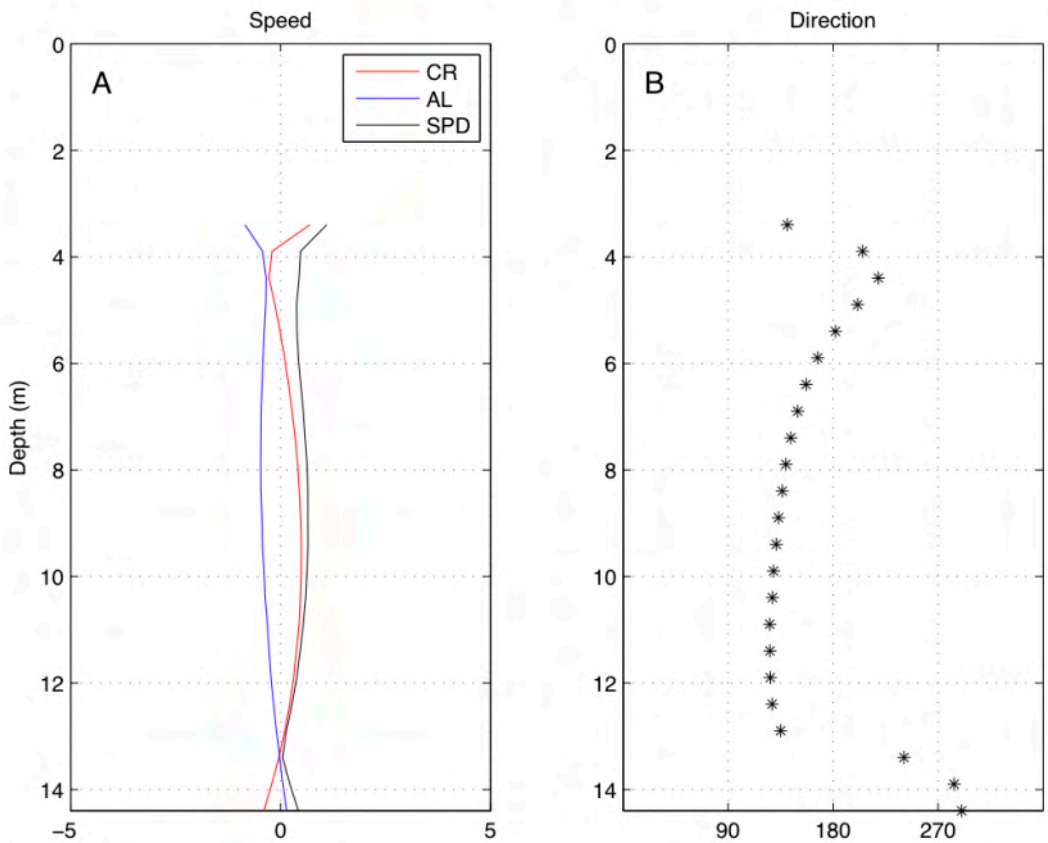

Figure 30. Profile plot of mean currents at the Inner Shelf site, Newport Beach, California, computed over the entire deployment period. A positive alongshore flow is directed upcoast, and a positive cross-shore flow is directed onshore. *A*, Mean alongshore, mean cross-shore and mean speed. *B*, Mean direction.

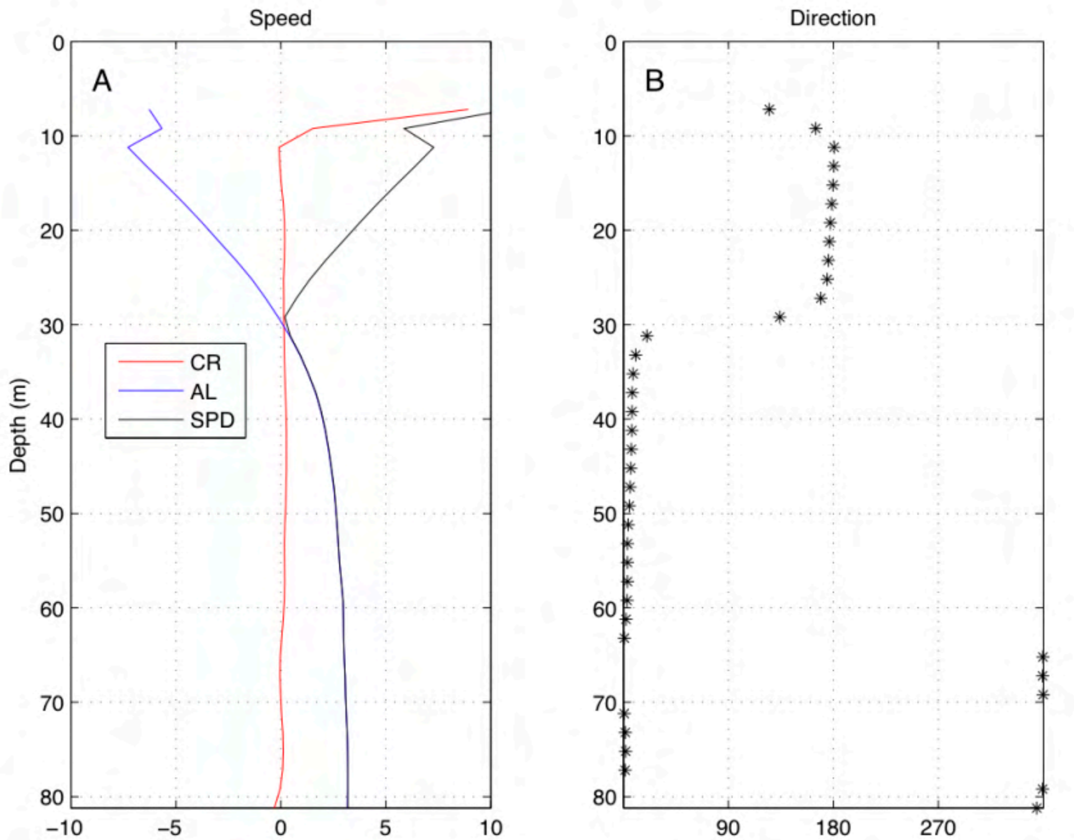

Figure 31. Profile plot of mean currents at the Shelf Break site, Newport Beach, California, computed over the entire deployment period. A positive alongshore flow is directed upcoast, and a positive cross-shore flow is directed onshore. *A*, Mean alongshore, mean cross-shore, and mean speed. *B*, Mean direction.

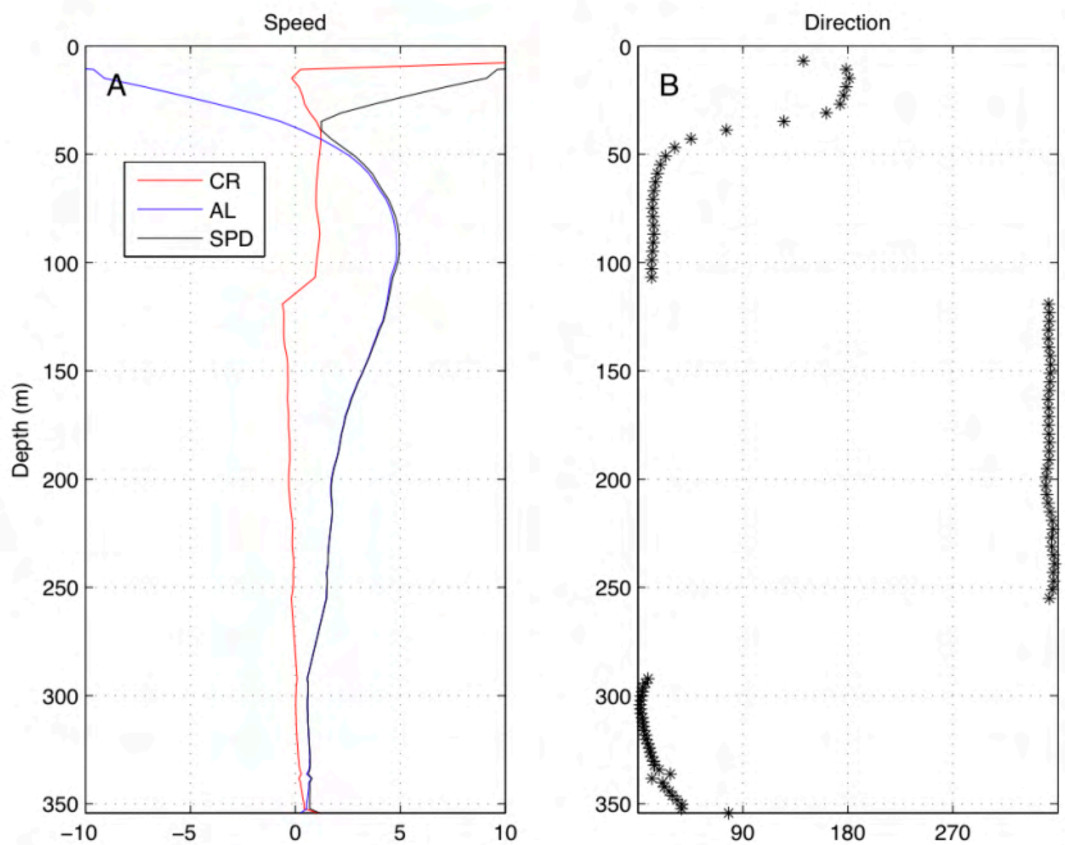

Figure 32. Profile plot of mean currents at the Slope site, Newport Beach, California, computed over the entire deployment period. A positive alongshore flow is directed upcoast, and a positive cross-shore flow is directed onshore. *A*, Mean alongshore, mean cross-shore, and mean speed. *B*, Mean direction.

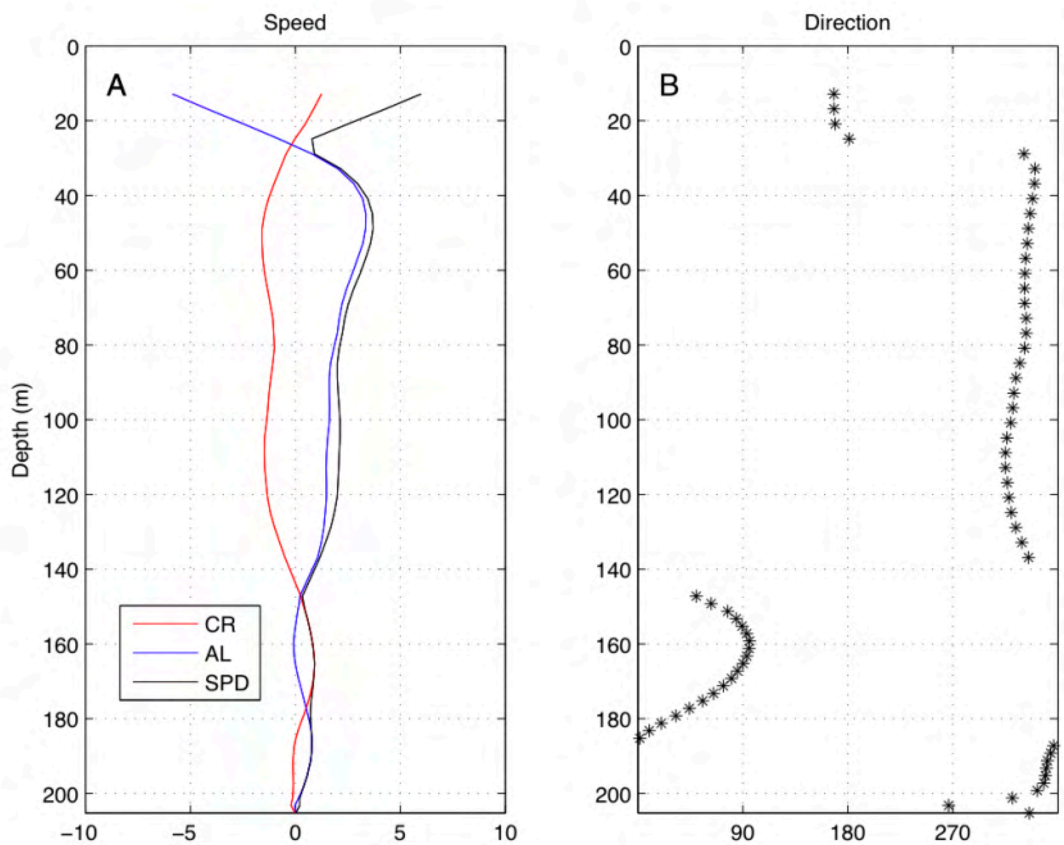

Figure 33. Profile plot of mean currents at the Shallow Canyon site, Newport Beach, California, computed over the entire deployment period. A positive alongshore flow is directed upcoast, and a positive cross-shore flow is directed onshore. *A*, Mean alongshore, mean cross-shore, and mean speed. *B*, Mean direction.

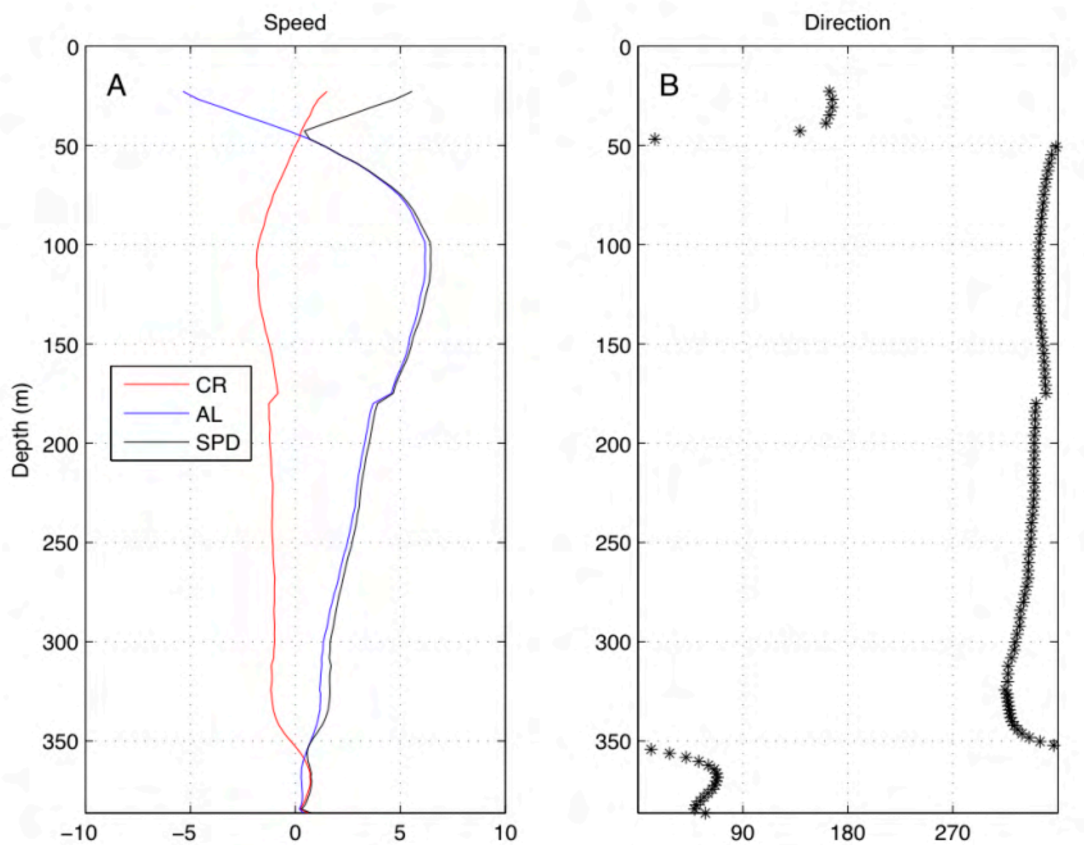

Figure 34. Profile plot of mean currents at the Deep Canyon site, Newport Beach, California, computed over the entire deployment period. A positive alongshore flow is directed upcoast, and a positive cross-shore flow is directed onshore. *A*, Mean alongshore, mean cross-shore, and mean speed. *B*, Mean direction.

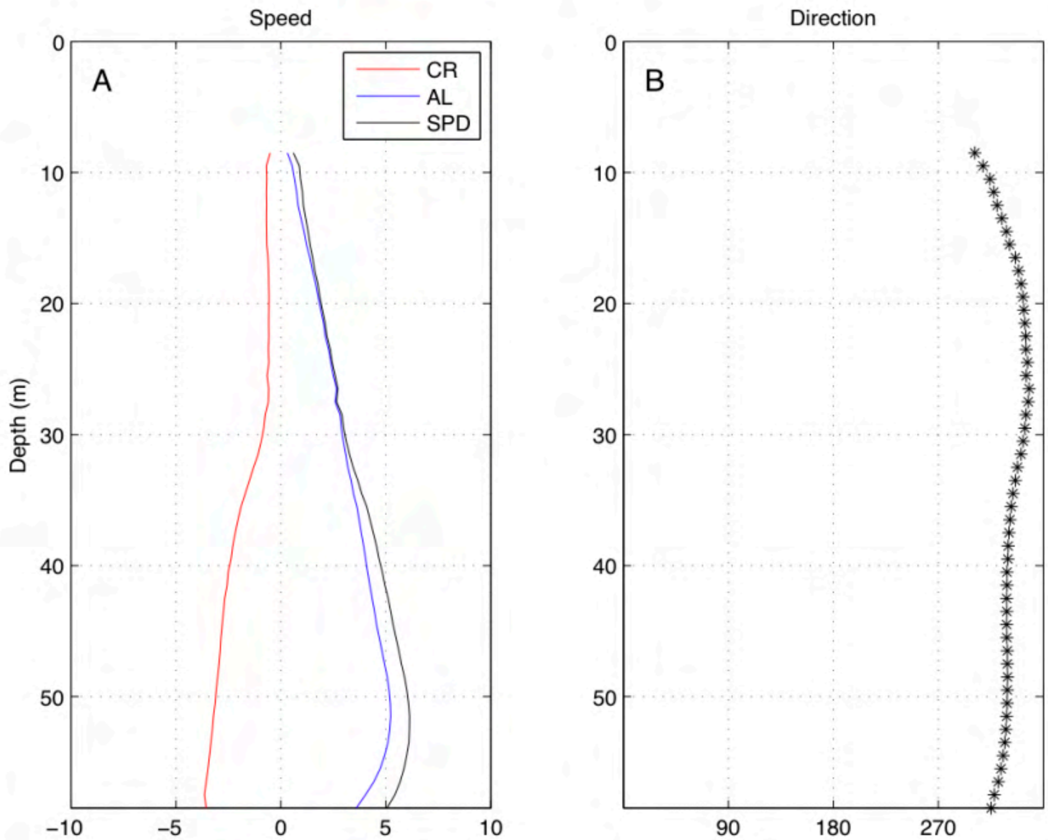

Figure 35. Profile plot of mean currents at the Orange County Sanitation District site M18, Newport Beach, California, computed over the entire deployment period. A positive alongshore flow is directed upcoast, and a positive cross-shore flow is directed onshore. *A*, Mean alongshore, mean cross-shore, and mean speed. *B*, Mean direction.

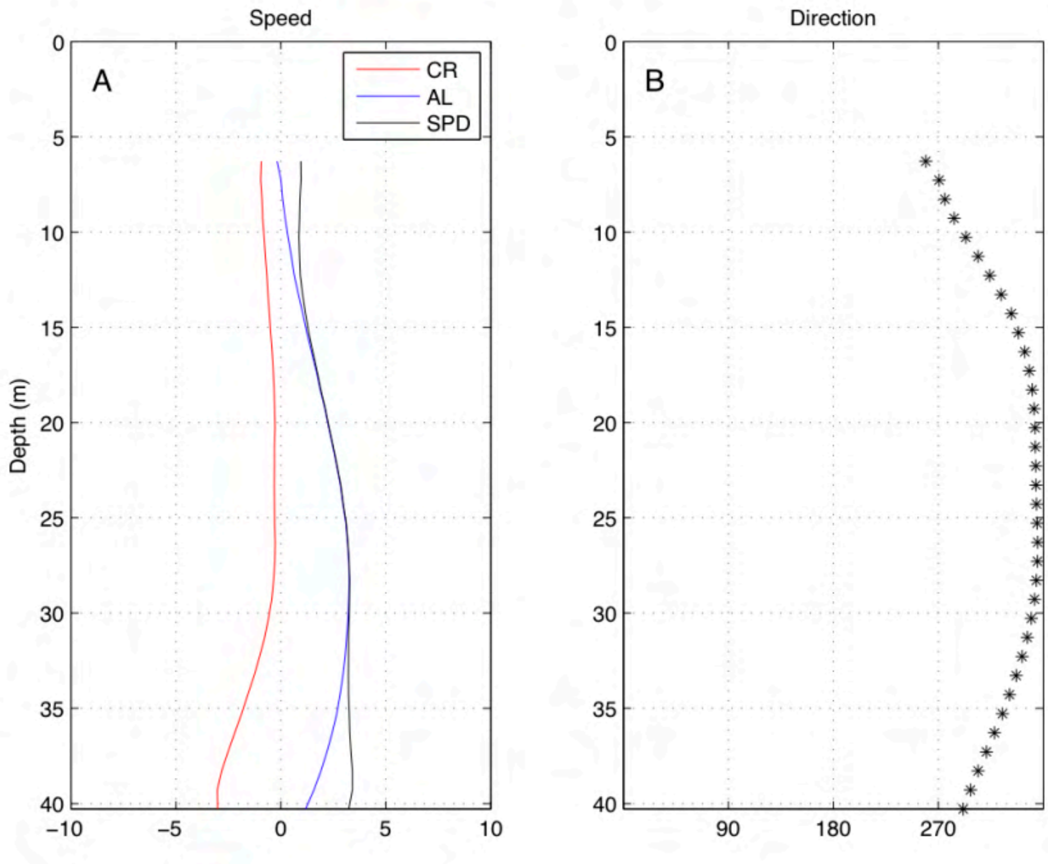

Figure 36. Profile plot of mean currents at the Orange County Sanitation District site M19, Newport Beach, California, computed over the entire deployment period. A positive alongshore flow is directed upcoast, and a positive cross-shore flow is directed onshore. *A*, Mean alongshore, mean cross-shore, and mean speed. *B*, Mean direction.

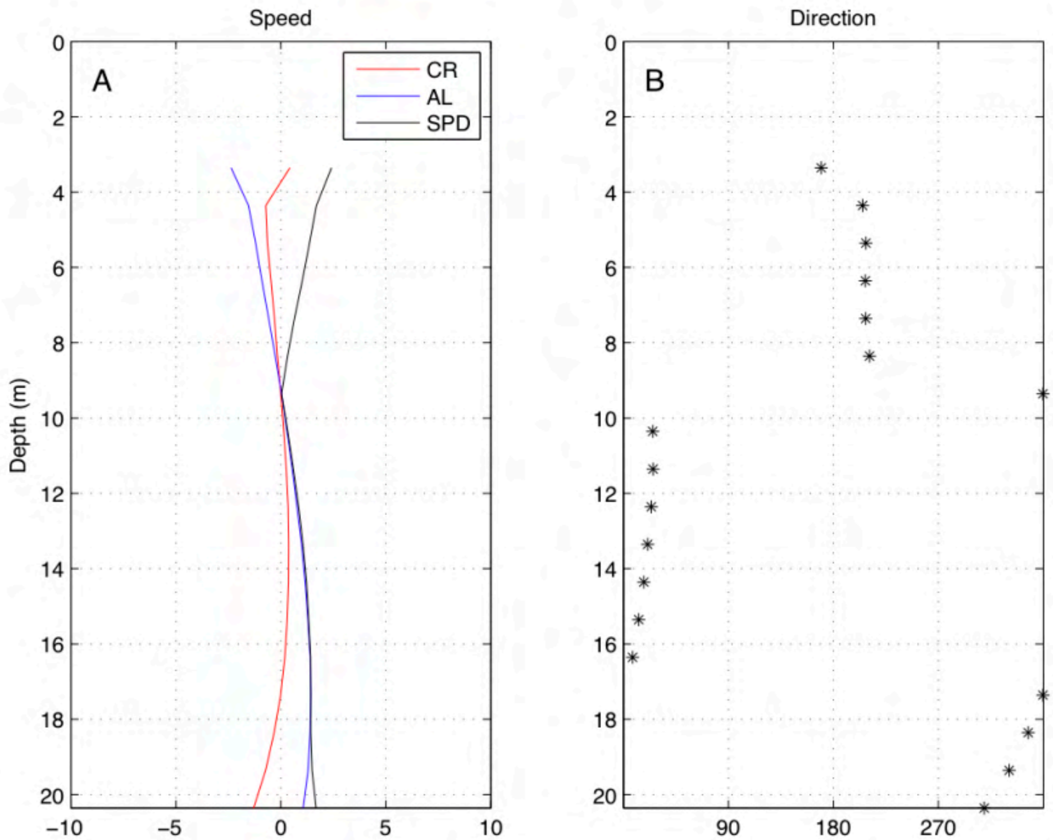

Figure 37. Profile plot of mean currents at the Orange County Sanitation District site M20, Newport Beach, California, computed over the entire deployment period. A positive alongshore flow is directed upcoast, and a positive cross-shore flow is directed onshore. *A*, Mean alongshore, mean cross-shore, and mean speed. *B*, Mean direction.

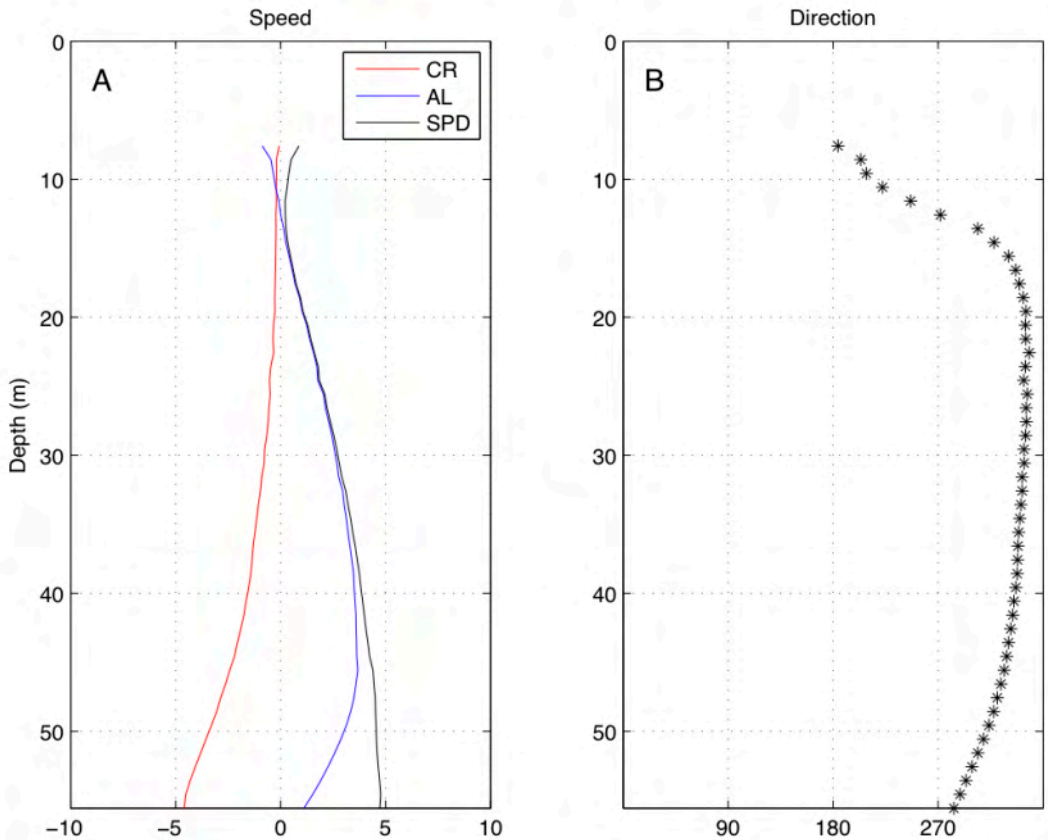

Figure 38. Profile plot of mean currents at the Orange County Sanitation District site M21, Newport Beach, California, computed over the entire deployment period. A positive alongshore flow is directed upcoast, and a positive cross-shore flow is directed onshore. *A*, Mean alongshore, mean cross-shore, and mean speed. *B*, Mean direction.

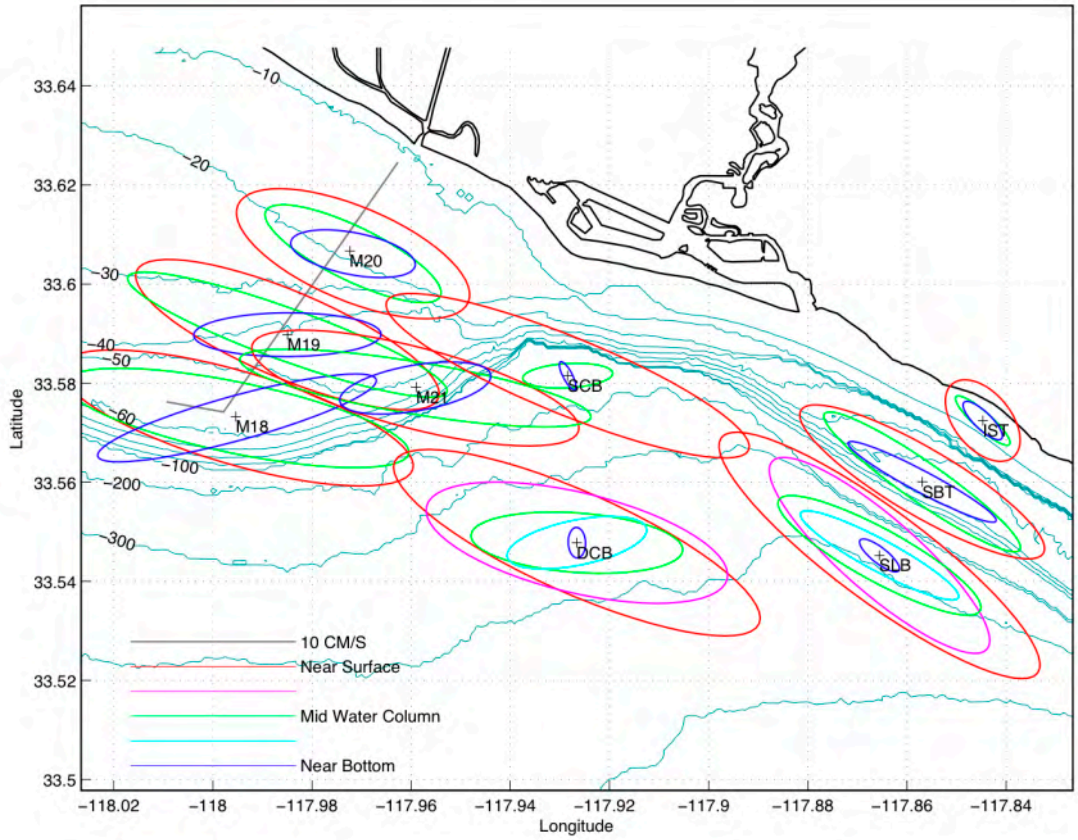

Figure 39. Map of the variance ellipses of the low-pass filtered flow from principal components analysis at several depth levels in the water column at each site, Newport Beach, California.

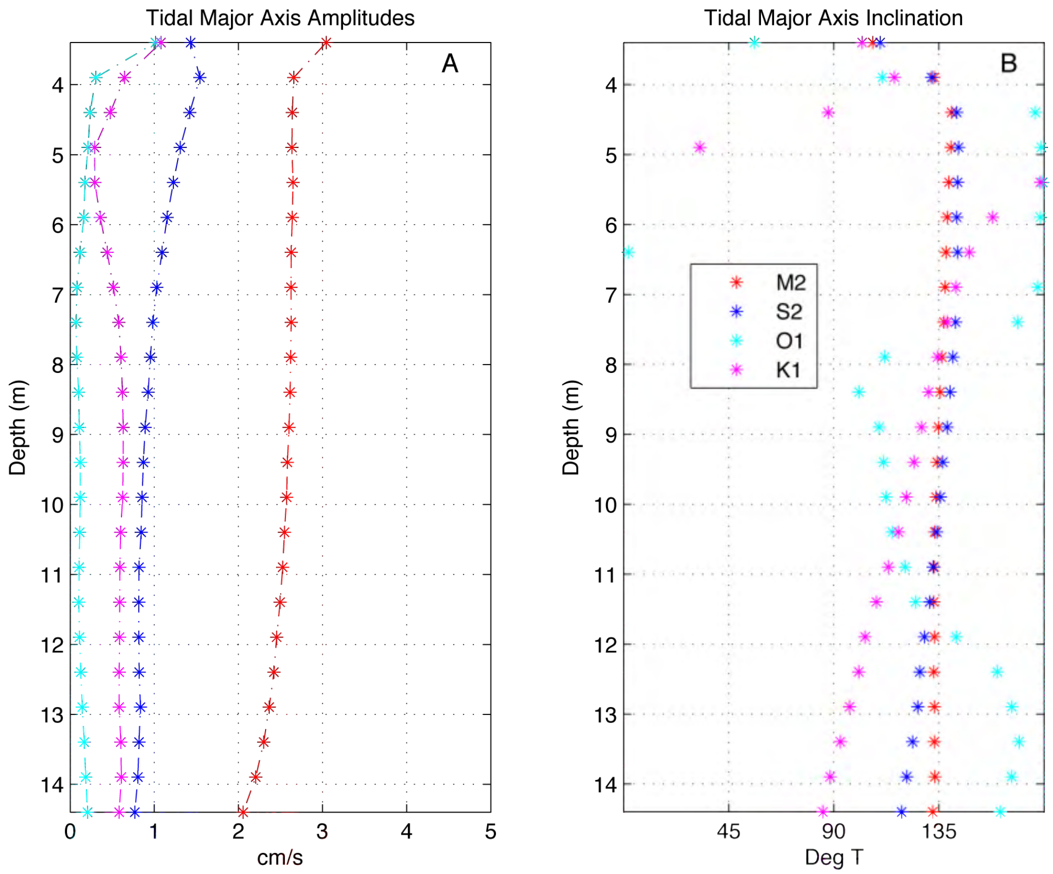

Figure 40. Profile of tidal currents at the Inner Shelf site, Newport Beach, California, computed over the entire deployment period. *A*, Major-axis ellipse amplitude. *B,* Major-axis inclination, in degrees clockwise from north.

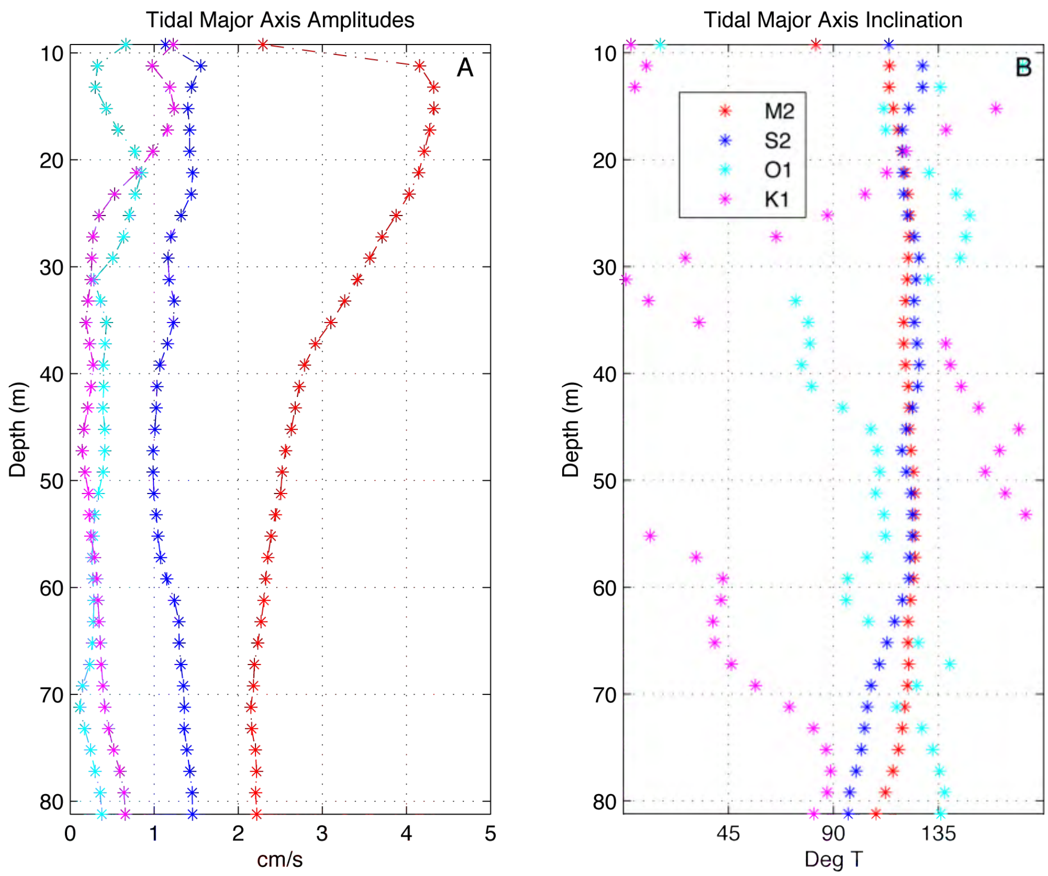

Figure 41. Profile of tidal currents at the Shelf Break site, Newport Beach, California, computed over the entire deployment period. *A*, Major-axis ellipse amplitude. *B*, Major-axis inclination, in degrees clockwise from north.

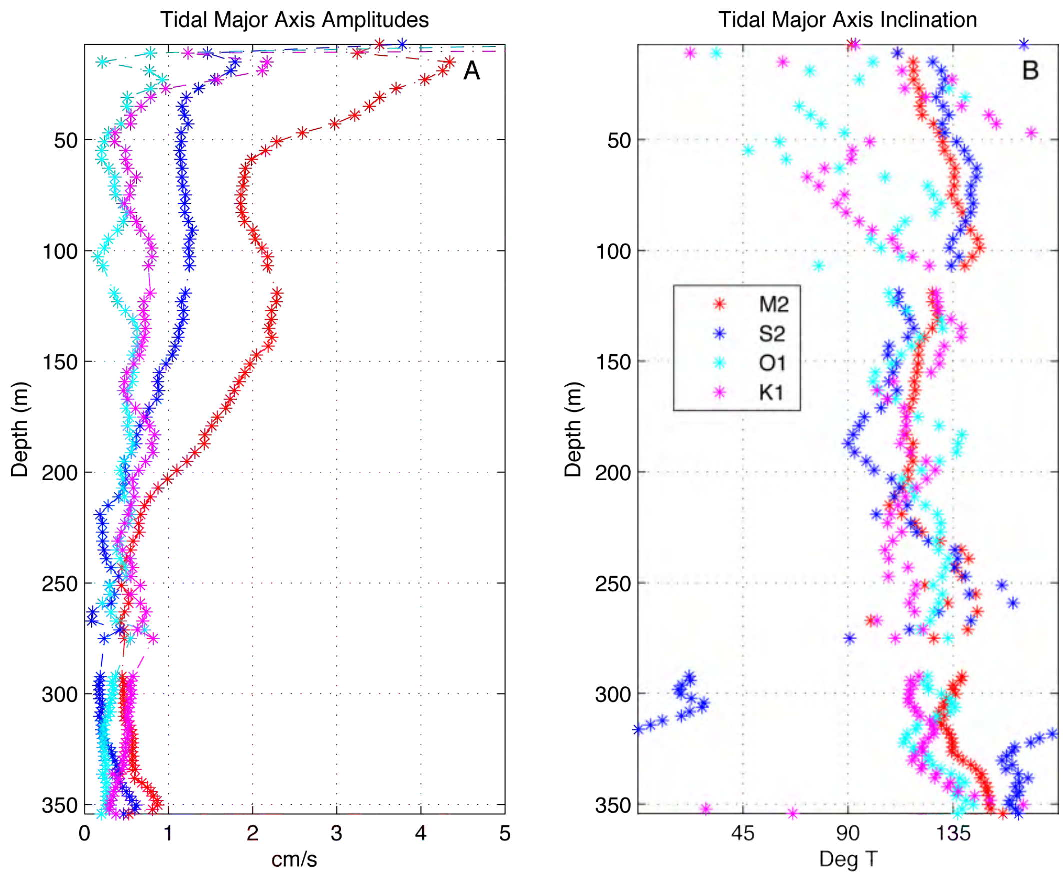

Figure 42. Profile of tidal currents at the Slope site, Newport Beach, California, computed over the entire deployment period. *A*, Major-axis ellipse amplitude. *B*, Major-axis inclination, in degrees clockwise from north.

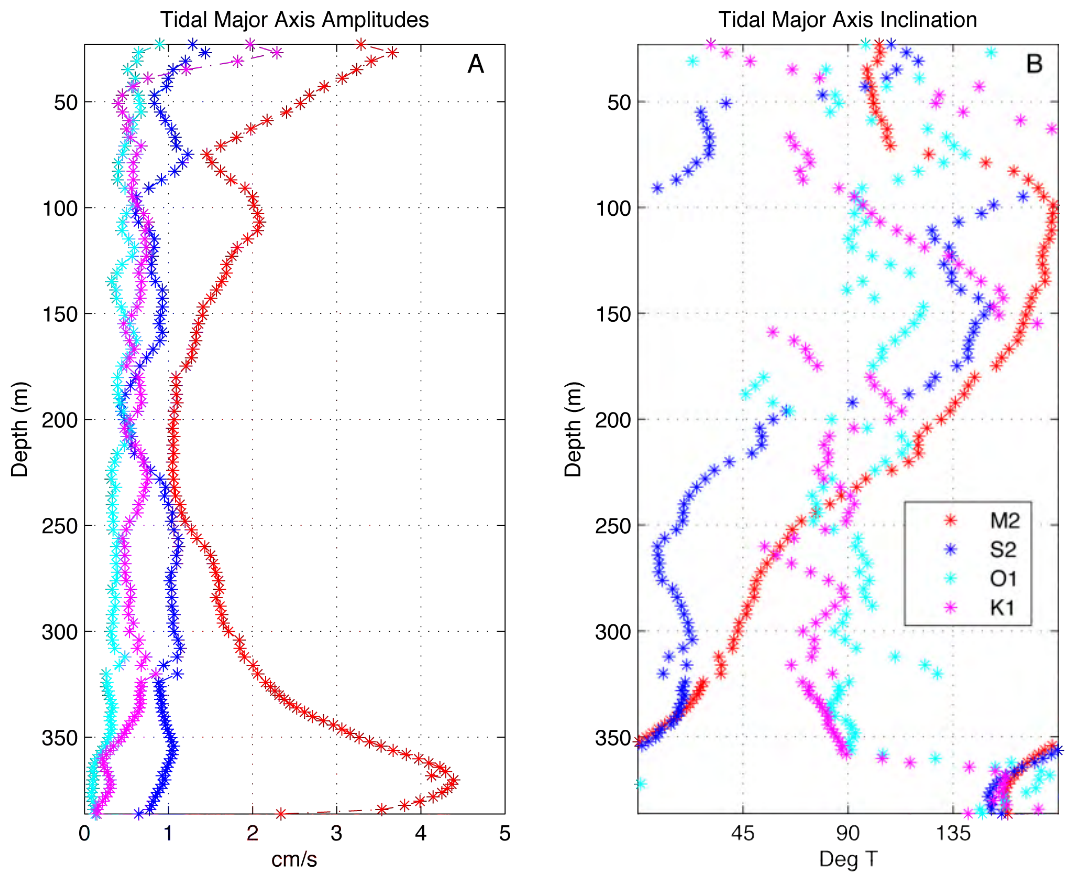

Figure 43. Profile of tidal currents at the Deep Canyon site, Newport Beach, California, computed over the entire deployment period. *A*, Major-axis ellipse amplitude. *B*, Major-axis inclination, in degrees clockwise from north.

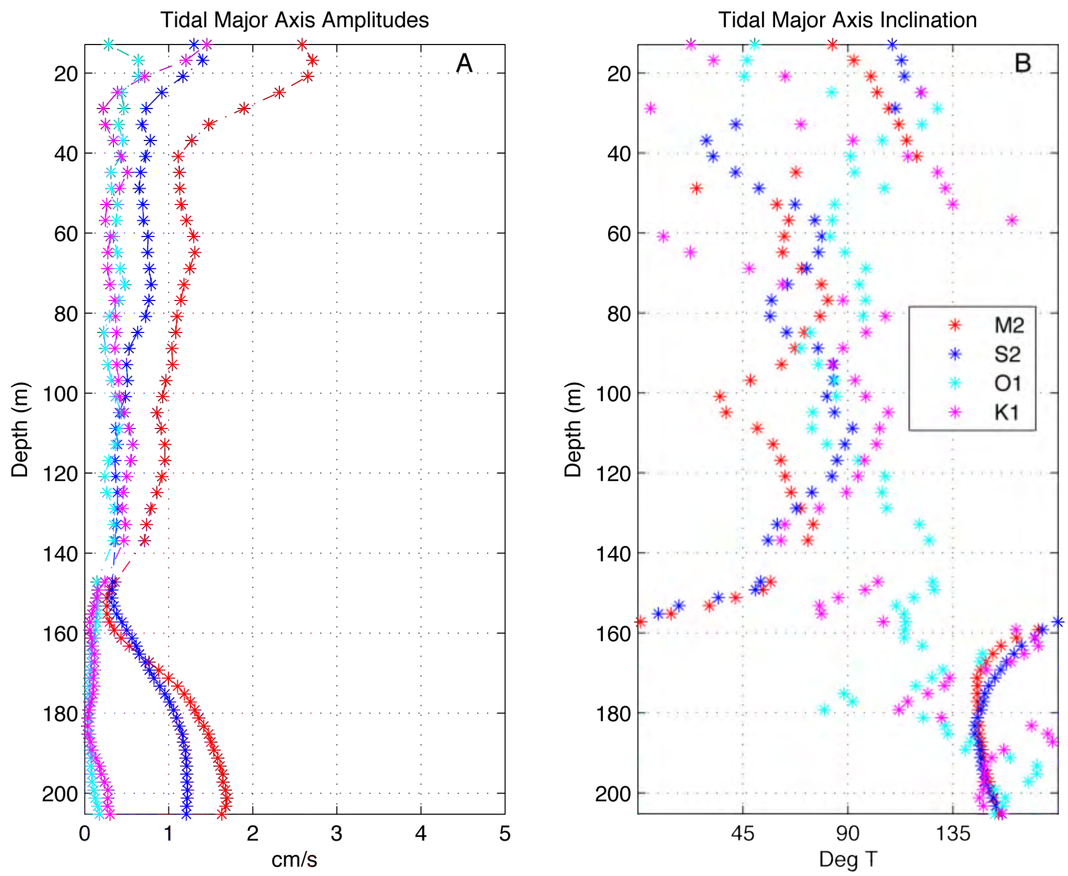

Figure 44. Profile of tidal currents at the Shallow Canyon site, Newport Beach, California, computed over the entire deployment period. A, Major-axis ellipse amplitude. B, Major-axis inclination, in degrees clockwise from north.

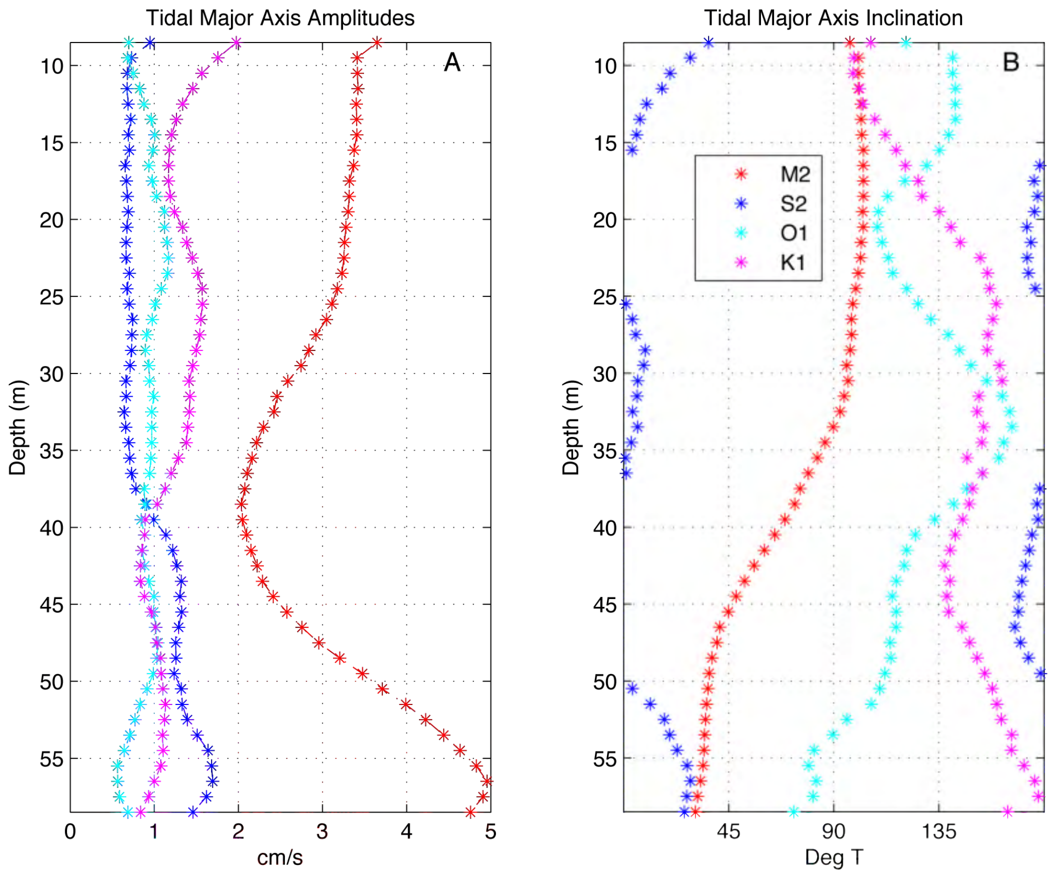

Figure 45. Profile of tidal currents at the Orange County Sanitation District site M18, Newport Beach, California, computed over the entire deployment period. *A*, Major-axis ellipse amplitude. *B*, Major-axis inclination, in degrees clockwise from north.

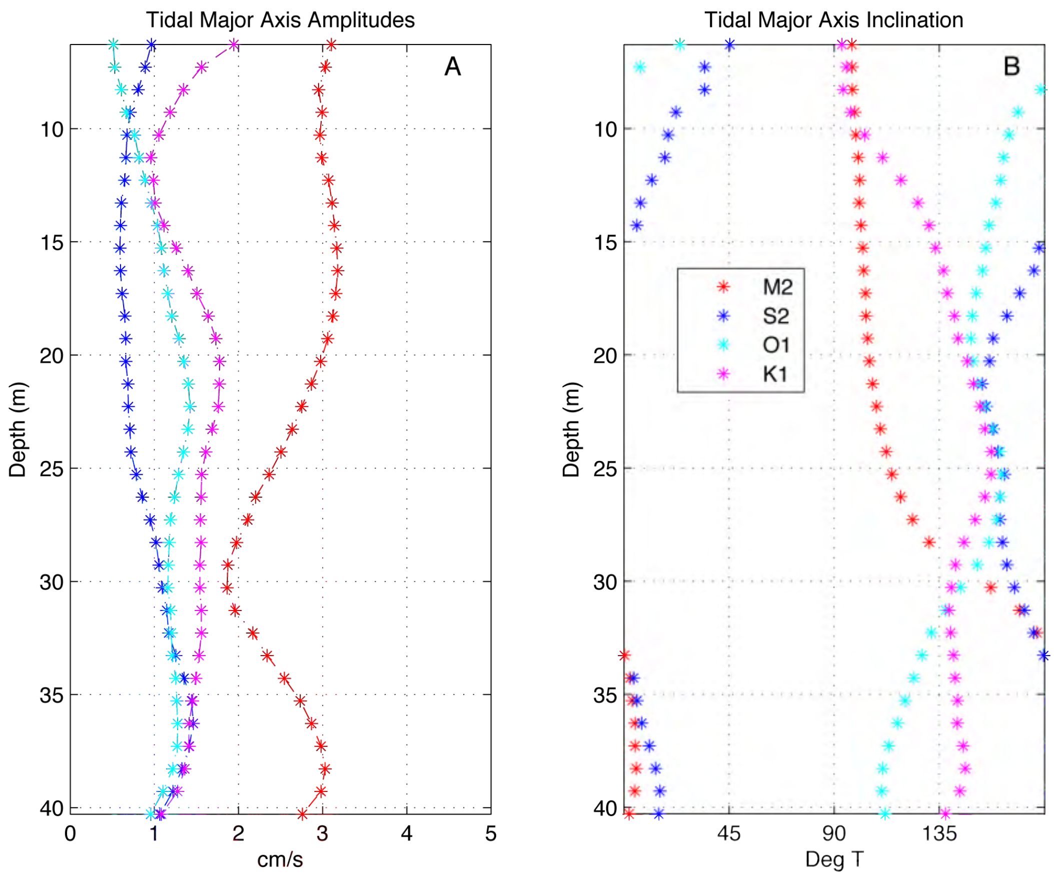

Figure 46. Profile of tidal currents at the Orange County Sanitation District site M19, Newport Beach, California, computed over the entire deployment period. *A*, Major-axis ellipse amplitude. *B*, Major-axis inclination, in degrees clockwise from north.

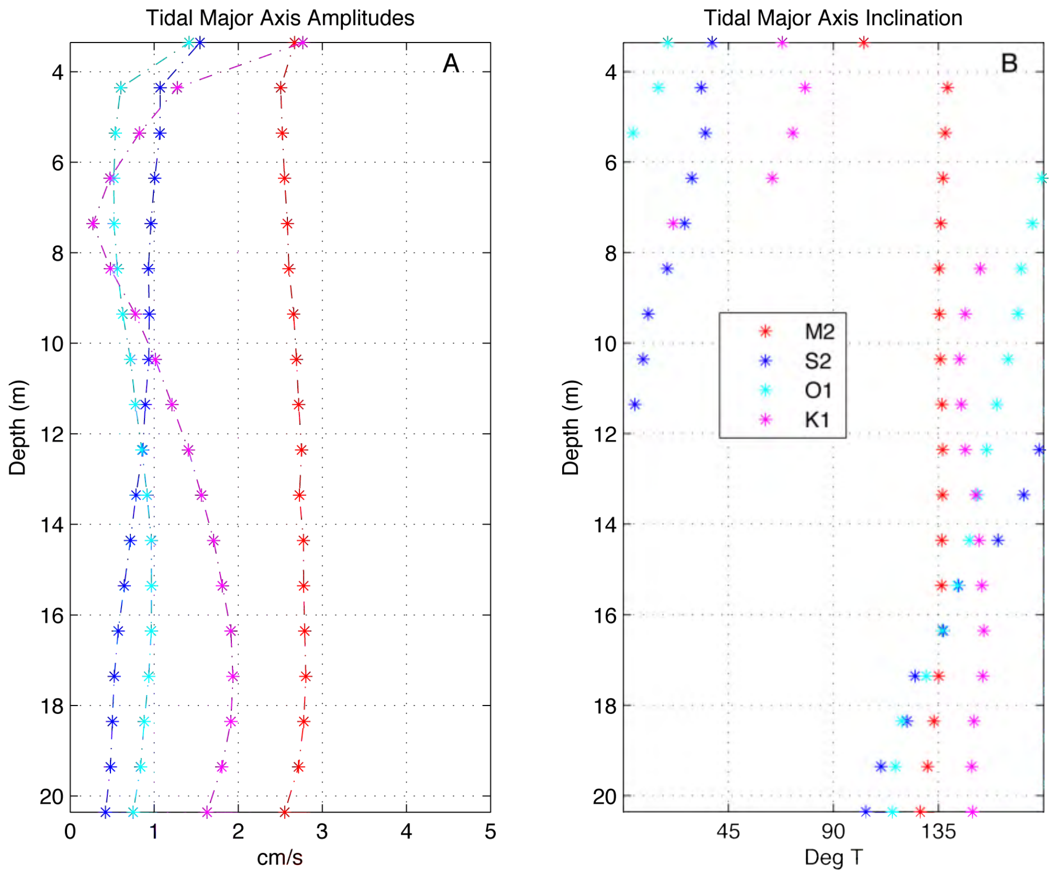

Figure 47. Profile of tidal currents at the Orange County Sanitation District site M20, Newport Beach, California, computed over the entire deployment period. *A*, Major-axis ellipse amplitude. *B*, Major-axis inclination, in degrees clockwise from north.

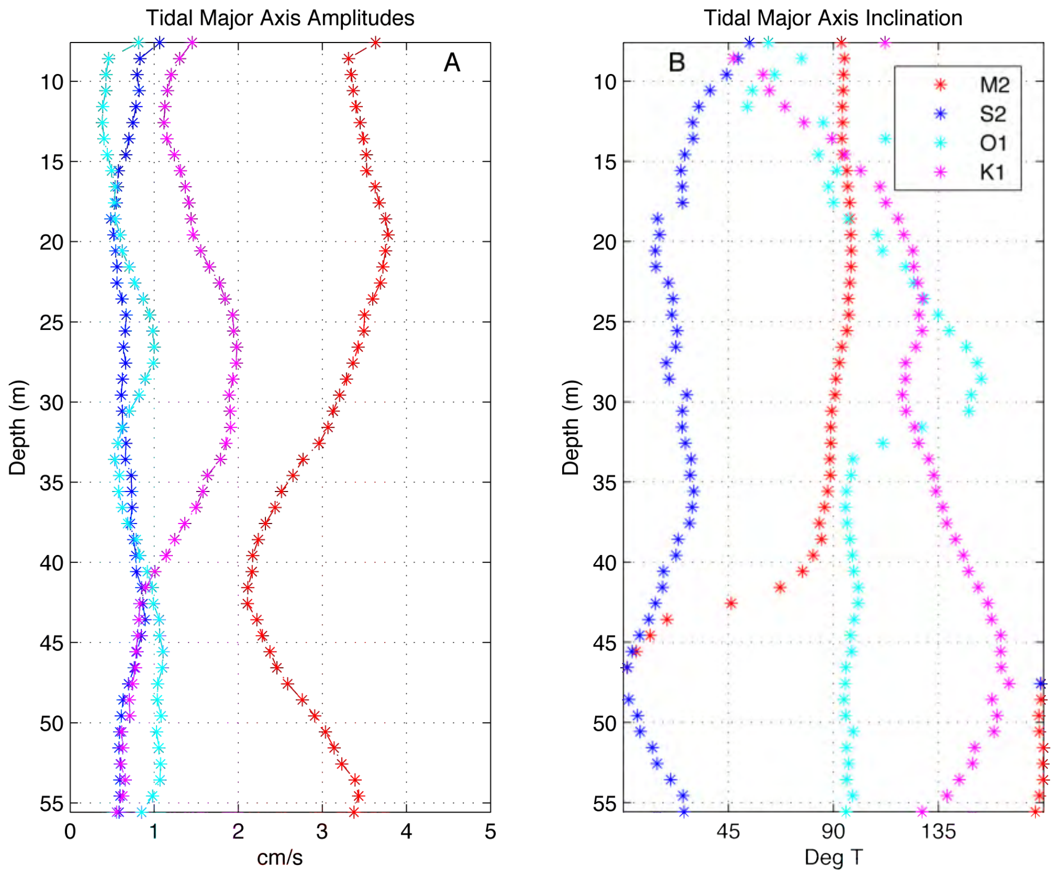

Figure 48. Profile of tidal currents at the Orange County Sanitation District site M21, Newport Beach, California, computed over the entire deployment period. *A*, Major-axis ellipse amplitude. *B*, Major-axis inclination, in degrees clockwise from north.

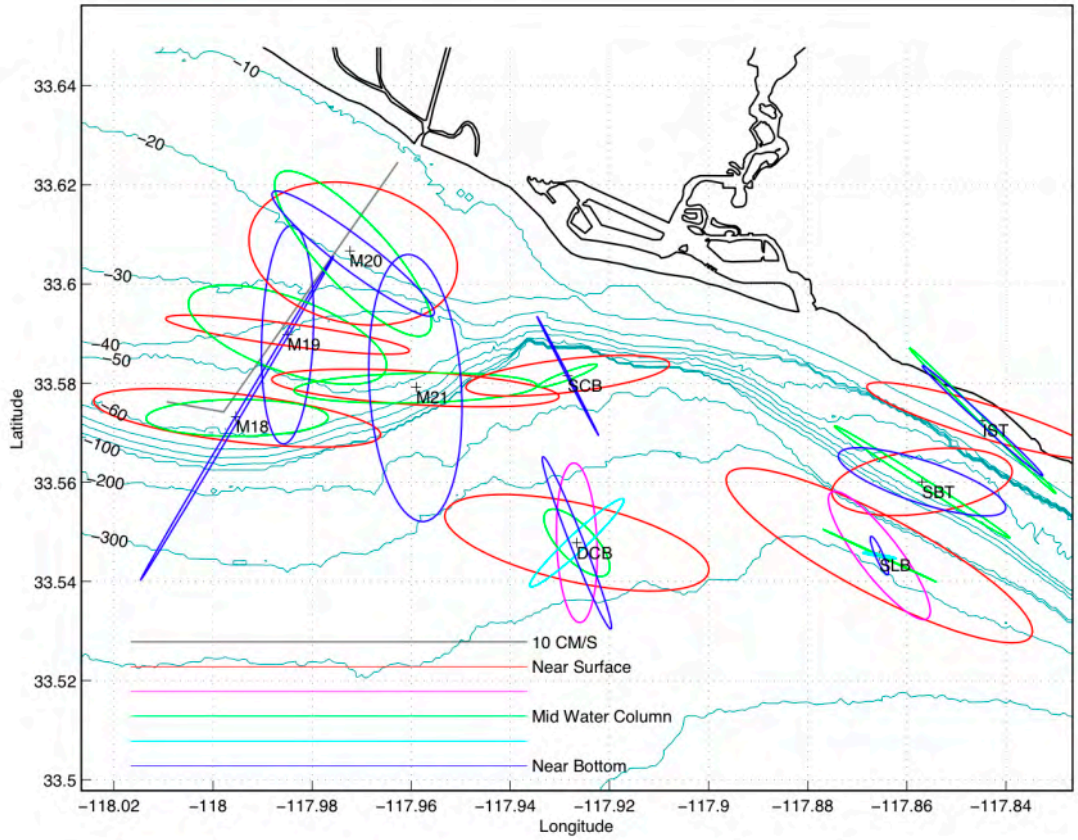

Figure 49. Map of the M_2 tidal ellipses calculated from a harmonic tidal analysis of the vector current-meter data at several depth levels in the water column, Newport Beach, California.

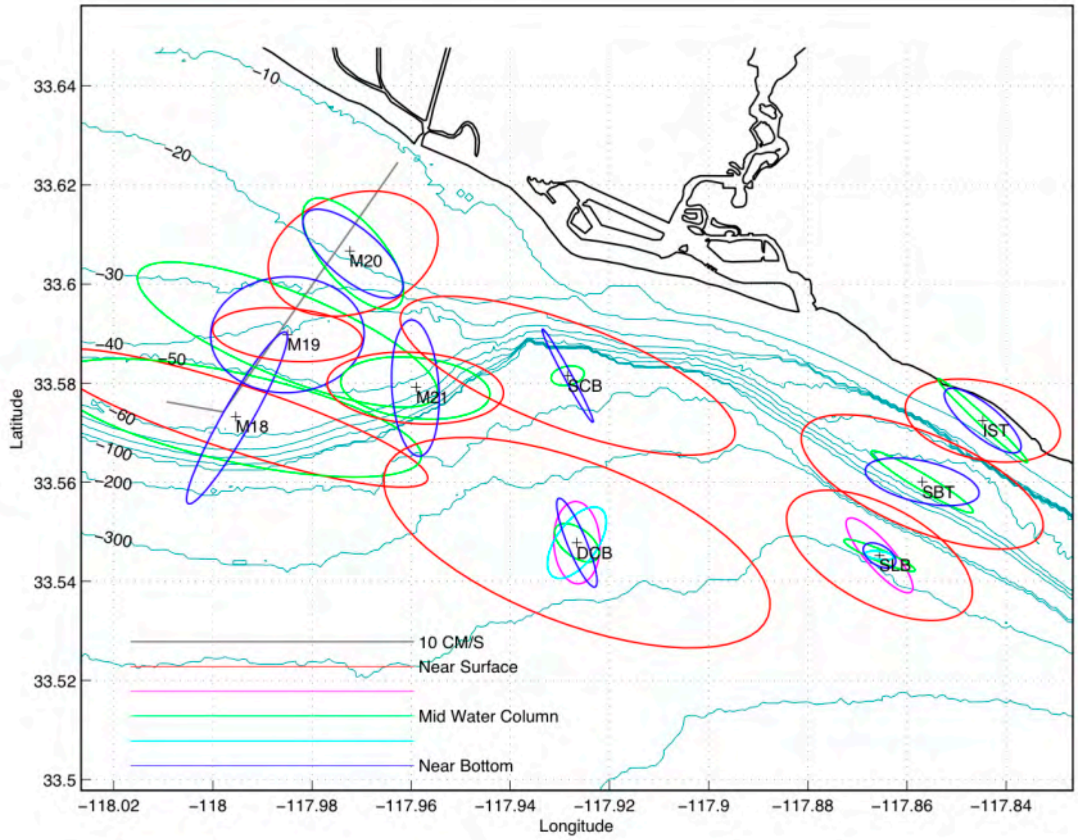

Figure 50. Map of the variance ellipses calculated from a principal components analysis of the harmonic tidal fit of the vector current-meter data at several depth levels in the water column, Newport Beach, California.